

London, 22<sup>nd</sup> September 2020

Dear Fortunat Joos (editor),

We included our responses to reviewer #3 below. We did not include a separate reply to reviewer #1, as the reviewer accepted the manuscript without changes.

Please find our revised manuscript including tracked changes below our response to reviewer #3. We added four additional photos to the supplementary information. Additionally, we added the four photos of the main text to the supplementary information to make them available in higher detail.

Thank you for your support in publishing our research at Biogeosciences.

Kind regards,

Tony Carr on behalf of the authors

## Uncertainties, sensitivities and robustness of simulated water erosion in an EPIC based global-gridded crop model

By T. W. Carr et al.

### 2<sup>nd</sup> Reply to Anonymous Referee #3

Dear reviewer,

Thank you again for your very helpful suggestions to improve our paper.

We added four additional photos to the supplementary information in addition to the photos of the main text. We appreciate your interest in the photos. However, we did not include all available photos to save a selection for additional publications. We added the location and slope information to each photo as detailed as possible, where it was recorded. But some photos were taken on excursions, in which we did not have the opportunity to record details about coordinates and topography.

Following your last suggestion, we added two sentences to line 548 addressing the need to collate soil erosion records for future research and referred to a recent publication focusing on this issue:

*“Moreover, the accessibility of field data should be improved as raw data is often not published or needs to be collected from numerous publications, grey literature and conference proceedings to obtain the large amount of data necessary for regional or global erosion studies. Therefore, we support recent efforts to collate erosion measurements and metadata from existing studies (Benaud et al., 2020) as we believe that the availability of field data through a single platform will greatly benefit future modelling studies and the understanding of soil erosion at all scales.”*

The reviewer’s comment is copied in purple below.

#### *Review of*

*Uncertainties, sensitivities and robustness of simulated water erosion in an EPIC-based global-gridded crop model*

*By T. W. Carr et al.*

*In general the authors have done an admirable job responding to the reviewers’ comments and the current manuscript is greatly improved compared to the previous version. I would be pleased to recommend this manuscript for publication following minor revision.*

*I particularly liked the authors additional sensitivity analyses concerning assumptions about which slopes are farmed. The test study for Italy showed clearly that if only low-slope landscapes are cultivated, very little soil erosion occurs. This result may form a basis for policymaking in some cases.*

*Responding to on my comments from the previous version, Figure 8 is a fantastic addition to the manuscript. I particularly appreciated the authors sharing of personal observations of (frequently unsustainable) cultivation practices in tropical mountains, and the illustration with photos. The figure showing years until total depletion of the soil profile (Fig. S10) is also very helpful.*

*I realize figure 8 is only a fraction of the photos you must have, and I liked seeing all of the photos that were provided in the response to reviewers document. I would be pleased if all of these additional photos could be provided in a supplementary materials document to accompany the final paper.*

*Furthermore, in figure 8, please provide approximate geographic coordinates and approximate elevation and slope for the sites shown in each of the four pictures. Exact numbers are not necessary, but it would be very helpful for future studies to examine these regions in more detail, e.g., using satellite and updated terrain data.*

*I realize that collation of a large database of soil erosion measurements would be beyond the scope of the current manuscript, and I fully appreciate the authors explanation of the challenges and effort that would be required to do this. I found the six points listed in the response to reviewers helpful information that could be used to form a basis for future international research initiatives. These may already be well known in the community. I would anyway request that the authors include a 1-2 sentence summary of the need and requirements for synthesizing soil erosion records in the final version of the paper, as this would be a very helpful citation, e.g., for anyone preparing a proposal to initiate or coordinate a project on the topic.*

# 1 **Uncertainties, sensitivities and robustness of simulated water** 2 **erosion in an EPIC-based global-gridded crop model** 3

4 Tony W. Carr<sup>1,\*</sup>, Juraj Balkovič<sup>2,3</sup>, Paul E. Dodds<sup>1</sup>, Christian Folberth<sup>2</sup>, Emil Fulajtar<sup>4</sup>,  
5 Rastislav Skalsky<sup>2,5</sup>

6 <sup>1</sup>University College London, Institute for Sustainable Resources, London, United Kingdom

7 <sup>2</sup>International Institute for Applied Systems Analysis, Ecosystem Services and Management Program,  
8 Laxenburg, Austria

9 <sup>3</sup>Department of Soil Science, Faculty of Natural Sciences, Comenius University in Bratislava, Bratislava,  
10 Slovak Republic

11 <sup>4</sup>International Atomic Energy Agency, Joint FAO/IAEA Division of Nuclear Techniques in Food and  
12 Agriculture, Vienna, Austria

13 <sup>5</sup>National Agricultural and Food Centre, Soil Science and Conservation Research Institute, Bratislava, Slovak  
14 Republic

15  
16 \* Correspondence to: Tony Carr ([tony.carr.16@ucl.ac.uk](mailto:tony.carr.16@ucl.ac.uk))  
17

18 **Abstract.** Water erosion on arable land can reduce soil fertility and agricultural productivity. Despite the impact  
19 of water erosion on crops, it is typically neglected in global crop yield projections. Furthermore, previous efforts  
20 to quantify global water erosion have paid little attention to the effects of field management on the magnitude of  
21 water erosion. In this study, we analyse the robustness of simulated water erosion estimates in maize and wheat  
22 fields between the years 1980 to 2010 based on daily model outputs from a global gridded version of the  
23 Environmental Policy Integrated Climate (EPIC) crop model. Using the MUSS water erosion equation and  
24 country-specific and environmental indicators determining different intensities in tillage, residue handling and  
25 cover crops, we obtained the global median water erosion rates of 7 t ha<sup>-1</sup> a<sup>-1</sup> in maize fields and 5 t ha<sup>-1</sup> a<sup>-1</sup> in wheat  
26 fields. A comparison of our simulation results with field data demonstrates an overlap of simulated and measured  
27 water erosion values for the majority of global cropland. Slope inclination and daily precipitation are key factors  
28 in determining the agreement between simulated and measured erosion values and are the most critical input  
29 parameters controlling all water erosion equations included in EPIC. The many differences between field  
30 management methods worldwide, the varying water erosion estimates from different equations and the complex  
31 distribution of cropland in mountainous regions add uncertainty to the simulation results. To reduce the  
32 uncertainties in global water erosion estimates, it is necessary to gather more data on global farming techniques,  
33 to reduce the uncertainty in global land use maps and to collect more data on soil erosion rates representing the  
34 diversity of environmental conditions where crops are grown.  
35

## 36 **1 Introduction**

37 Water erosion is widely recognized as a threat to global agriculture (den Biggelaar et al., 2004; Kaiser, 2004;  
38 Panagos et al., 2018; Pimentel, 2006). The removal of topsoil by surface runoff reduces soil fertility and crop

39 yields due to loss of nutrients, degradation of the soil structure, and decreasing plant-available water capacity  
40 (Våje et al., 2005). Water erosion is a natural process, but the impact of agricultural field management on surface  
41 cover and roughness is decisive for the magnitude of water erosion. High energy precipitation, steep slopes and  
42 lack of vegetation cover intensify water erosion. The most vulnerable areas are mountainous regions, due to steep  
43 slopes, the tropics and subtropics, due to abundant high energy precipitation, and arid regions, where precipitation  
44 events are rare but often intense and the vegetation cover is sparse. This global distribution of water erosion is  
45 indicated by suspended sediment in rivers (Walling and Webb, 1996). South America, Sub-Saharan Africa, South  
46 and East Asia have been identified as the most vulnerable regions to erosion on agricultural land by several prior  
47 studies (Borrelli et al., 2017; Pimentel et al., 1995).

48 Despite its importance for global agriculture, water erosion is usually not considered in global gridded crop model  
49 (GGCM) studies. Throughout the past decade, GGCMs - typically combinations of agronomic or ecosystem  
50 models and global gridded input data infrastructures - have become essential tools for climate change impact  
51 assessments, evaluations of agricultural externalities, and as input data providers for agro-economic models  
52 (Mueller et al., 2017). Few assessments have considered land degradation processes and found their inclusion and  
53 understanding crucial for evaluating climate change mitigation and adaptation strategies (Balkovič et al., 2018;  
54 Chappell et al., 2016). Beyond crop models, there is a need to improve the representation of agricultural  
55 management and soil-related processes in earth system models to better reflect carbon sinks and sources (Luo et  
56 al., 2016; McDermid et al., 2017; Pongratz et al., 2018). Moreover, improving the representation of water erosion  
57 in large-scale models is urgently needed to inform major environmental and agricultural policy programs such as  
58 the European Union's Common Agricultural Policy (CAP), the United Nations Sustainable Development Goals  
59 (SDGs), the United Nations Convention to Combat Desertification (UNCCD) and the Intergovernmental Science-  
60 Policy Platform on Biodiversity and Ecosystem Services (IPBES) (Alewell et al., 2019). Yet, the necessary  
61 algorithms to simulate water erosion are often not incorporated in such models. Exceptions among field-scale crop  
62 models, which are frequently used in GGCM ensemble studies, are the Environmental Policy Integrated Climate  
63 model (EPIC) and Agricultural Production Systems Simulator (APSIM). Compared to other commonly used crop  
64 models in GGCMs, EPIC stands out in its detailed representation of soil processes including water erosion and  
65 the impacts of tillage on soil properties (Folberth et al., 2019).

66 Recently, water erosion models such as the Universal Soil Loss Equation (USLE) and the Revised Universal Soil  
67 Loss Equation (RUSLE) have been used to estimate global water erosion. Annual global soil removal estimates  
68 and water erosion rates on cropland of recent studies range between 13 – 22 Gt and 11 - 13 t ha<sup>-1</sup> (Borrelli et al.,  
69 2017; Doetterl et al., 2012; van Oost et al., 2007). USLE and its modifications were developed in the Midwestern  
70 United States and should ideally be evaluated against soil erosion measurements when used for other agro-  
71 environmental zones (Evans and Boardman, 2016). However, the uneven distribution of field data around the  
72 world, the lack of long-term soil measurements in most global regions, and the great variability of the designs of  
73 erosion rate measurements hamper the evaluation of global soil loss estimates derived from models (Auerswald  
74 et al., 2004; Borrelli et al., 2017; García-Ruiz et al., 2015). In addition, model input data on topography, soil  
75 properties and land use are often aggregated over large areas and thus simulation results cannot be directly  
76 compared to single field measurements at specific locations.

77 Most global soil removal estimates using water erosion models are based on static observation approaches or on  
78 very coarse timescales that do not fall below annual time steps (Borrelli et al., 2017). Therefore, seasonal patterns  
79 of soil cover and precipitation intensities are neglected even though they are crucial factors for water erosion. The  
80 state of the soil and its cover is influenced by land management, such as the choice of crops, planting and harvest  
81 dates, tillage and plant residue management. Accordingly, neglecting the impact of seasonal changes in vegetation  
82 cover and field management practices constitutes large uncertainty in global water erosion estimates. Crop models  
83 usually simulate crop growth on a daily timescale, which allows attached water erosion models to account for  
84 daily changes in weather, soil properties and vegetation cover. However, uncertainty remains due to the increasing  
85 requirement of input data for daily simulations, which is especially challenging at a global scale.

86 The overall aim of this study is (i) to analyse the robustness of water erosion estimates in all global agro-  
87 environmental regions simulated with an EPIC-based global-gridded crop model and (ii) to discuss the main  
88 drivers affecting the robustness and the uncertainty of simulated water erosion rates on a global scale. We simulate  
89 global water erosion rates in maize and wheat fields using different empirical erosion equations in EPIC while  
90 accounting for the daily crop growth and development under different field management scenarios. Here, maize  
91 and wheat are used as representative crops of global agriculture, as they are grown under most environmental  
92 conditions and represent contrasting soil cover patterns. Our global simulations are carried out for a baseline crop  
93 management scenario based on a set of environmental and country-specific assumptions and indicators, which is  
94 a common practice in global gridded crop modelling. In addition, we quantify the uncertainties of simulated water  
95 erosion values stemming from (i) uncertain field management inputs, and (ii) water erosion calculation methods.  
96 We also evaluate the model's sensitivity to all inputs involved in the water erosion calculation to interpret the  
97 variability and uncertainties of the simulation results, and to discuss the differences between water erosion  
98 equations. Finally, we use field measurements from various locations world-wide to evaluate the robustness of  
99 estimated water erosion rates under different environmental conditions.

## 100 **2 Methods**

101 The simplified framework in Figure 1 illustrates the particular stages of the methodological procedure applied by  
102 this study and their relationships to input data and model outputs. Both, input and output data are used twofold.  
103 We use input data (i) to simulate daily maize and wheat growth and water erosion with EPIC, and (ii) to analyse  
104 the sensitivity of relevant model parameters to simulate global water erosion with all equations in EPIC. We use  
105 model outputs (i) to calculate a baseline global water erosion scenario, and (ii) to address the uncertainty of  
106 simulation results. The final step of this study consists of the robustness check of the model outputs using field  
107 data. A detailed description of each element of this study is described in the following sections.

108

### 109 **2.1 Modelling water erosion and crop growth with EPIC**

#### 110 **2.1.1 Global gridded crop model and input data**

111 We use a global gridded version of the Environmental Policy Integrated Climate (EPIC) crop model, EPIC-IIASA  
112 (Balkovič et al., 2014), to simulate soil sediment loss with runoff from 1980 to 2010 while accounting for the  
113 daily growth of maize and wheat under different field management scenarios. EPIC can simulate the growth of a  
114 wide range of crops and has a sophisticated representation of carbon, nutrient and water dynamics as well as a

115 wide variety of possible field management options, including tillage operations and crop rotations (Izaurre et al., 2006; Sharpley and Williams, 1990). Originally EPIC was named Erosion-Productivity Impact Calculator and  
116 was developed to determine the relationship between erosion and soil productivity. Due to its origin, EPIC has  
117 several options to calculate water erosion caused by precipitation, runoff and irrigation (Williams, 1990).  
118

119 EPIC-IIASA requires global soil and topography data and daily weather data. The basic spatial resolution of the  
120 model is 5' x 5' at which soil and topographic data are provided. These are aggregated to homogenous response  
121 units and further intersected with a 30' x 30' climate grid, the resolution at which global gridded climate data are  
122 available. This results in a total of 131,326 grid cells with a spatial resolution ranging between 5' to 30' (about 9  
123 km to 56 km near the equator) (Skalský et al., 2008). We use global daily weather data from the AgMERRA  
124 dataset for the years 1980-2010 (Ruane et al., 2015), soil information from the Harmonized World Soil Database  
125 (FAO/IIASA/ISRIC/ISSCAS/JRC, 2009), and topography from USGS GTOPO30 (USGS, 1997). Each grid cell  
126 is represented by a single field characterized by the combination of topography and soil conditions prevailing in  
127 this landscape unit. Each representative field has a defined slope length (20 – 200 m) and field size (1 - 10 ha)  
128 based on a set of rules for different slope classes (Table S1). The slope of each representative field is determined  
129 by the slope class covering the largest area in each grid cell (Table S1). Slope classes are taken from a global  
130 terrain slope database (IIASA/FAO, 2012) and are based on a high-resolution 90 m SRTM digital elevation model.  
131 In each grid cell, we consider reported growing seasons for maize and wheat (Sacks et al., 2010), and spatially  
132 explicit nitrogen and phosphorus fertilizer application rates (Mueller et al., 2012).

### 133 2.1.2 Water erosion equations

134 EPIC includes seven empirical equations to calculate water erosion (Wischmeier and Smith, 1978). The basic  
135 equation is:

$$136 Y = R * K * LS * C * P \quad (1)$$

137 where Y is soil erosion in t ha<sup>-1</sup> (mass/area), R is the erosivity factor (erosivity unit/area), K is the soil erodibility  
138 factor in t MJ<sup>-1</sup> (mass/erosivity unit), LS is the slope length and steepness factor (dimensionless), C is the soil  
139 cover and management factor (dimensionless) and P is the conservation practices factor (dimensionless).

140 The main difference between the water erosion equations available in EPIC is their energy components used to  
141 calculate the erosivity factor. The USLE, RUSLE and RUSLE2 equations use precipitation intensity as an erosive  
142 energy to calculate the detachment of soil particles. The Modified Universal Soil Loss Equation (MUSLE)  
143 equation and its variations MUST and MUSS use runoff variables to simulate water erosion and sediment yield.  
144 The Onstad-Foster equation (AOF) combines energy through rainfall and runoff (Table 1).

145 The erosion energy component is calculated as a function of either runoff volume Q (mm), peak runoff rate q<sub>p</sub>  
146 (mm h<sup>-1</sup>) and watershed area WSA (ha), or via the rainfall erosivity index EI (MJ ha<sup>-1</sup>). The latter determines the  
147 detachment of soil particles through the energy of daily precipitation and a statistical estimate of the daily  
148 maximum intensity of precipitation falling within 30 minutes. RUSLE2 is the only equation calculating soil  
149 deposition. If the sediment load exceeds the transport capacity, determined by a function of flow rate and slope  
150 steepness, soil is deposited, which is calculated by a function of flow rate and particle size (USDA-ARC, 2013).

151 The soil cover and management factor is updated for every day where runoff occurs using a function of crop  
152 residues, biomass cover and surface roughness. The impact of soil erodibility on simulated water erosion is  
153 calculated for the top-soil layer at the start of each simulation year as a function of sand, silt, clay and organic  
154 carbon content. The topographic factor is calculated as a function of slope length and slope steepness. A detailed  
155 description of the cover and management, soil erodibility and topographic factor is provided in the supporting  
156 information (Text S1). The conservation practice factor is included in all equations as a static coefficient ranging  
157 between 0 and 1, where 0 represents conservation practices that prevent any erosion and 1 represents no  
158 conservation practices. Typical conservation practice factors can be derived from tables, which include values  
159 ranging from 0.01 to 0.35 for terracing strategies and from 0.25 to 0.9 for different contouring practices (Morgan,  
160 2005; Wischmeier and Smith, 1978). Alternatively, values can be derived from local field studies and remote  
161 sensing (Karydas et al., 2009; Panagos et al., 2015), from equations using topographical data (Fu et al., 2005;  
162 Terranova et al., 2009), or from economic indicators (Scherer and Pfister, 2015).

### 163 **2.1.3 Field management scenarios**

164 Field management techniques influencing soil properties and soil cover have a significant impact on the amount  
165 of water erosion. However, these methods are very heterogenous around the world and data on different field  
166 management techniques are sparse. Therefore, three tillage management scenarios – conventional tillage, reduced  
167 tillage and no-tillage – were designed by altering parameters related to water erosion to analyse the impact of field  
168 management on simulated water erosion and to draw conclusions on its impact on the quality of simulation results.

169 In the reduced and no-tillage scenarios, we decrease soil disturbance by reducing cultivation operations, tillage  
170 depth and surface roughness, and we increase plant residues left in the field after harvest. In addition, we reduce  
171 the runoff curve numbers, which indicate the runoff potential of a hydrological soil group, land use and treatment  
172 class, with decreasing tillage intensification by using pre-defined values for the cover treatment classes presented  
173 in Table 2 (Sharpley and Williams, 1990). By lowering the runoff curve numbers, the impact of reduced tillage  
174 practices on the hydrologic balance can be taken into account (Chung et al., 1999). We simulate each tillage  
175 scenario with and without green fallow cover in between growing seasons, leading to a total of six field  
176 management scenarios.

## 177 **2.2 Baseline scenario for estimating global water erosion in wheat and maize fields**

178 We estimate the rate of water erosion globally by combining these six tillage and cover crop scenarios in different  
179 regions of the world, using climatic and country-specific assumptions and indicators (Table 3). We chose maize  
180 and wheat as two contrasting crop types for analysing water erosion in different cultivation systems. Maize is a  
181 row crop with relatively large areas of bare and unprotected soil between the crop rows. The plant density in wheat  
182 fields is much higher, which improves the protection of soils against water erosion.

183 We consider conventional and reduced tillage systems globally while considering no-tillage only for countries in  
184 which the share of conservation agriculture is at least 5 %. In tropical regions, we simulate water erosion with a  
185 green cover in between maize and wheat seasons to account for soil cover from a year-round growing season. In  
186 temperate and snow regions, we simulate water erosion affected by both soil cover throughout the year and bare  
187 soil in winter seasons. In arid regions, we do not simulate green cover in between growing seasons due to the  
188 limited water supply.



189 On slopes steeper than 5 %, we consider only rainfed agriculture, as hilly cropland is irrigated predominantly on  
190 terraces that prevent water runoff. To account for erosion control measures on steep slopes, we use a conservation  
191 P-factor of 0.5 on slopes steeper than 16 %, and a P-factor of 0.15 on slopes steeper than 30 % to simulate  
192 contouring and terracing based on the range of P-values presented by Morgan (2005). The threshold for slopes  
193 that are cultivated with conservation practices is based on the slope classes used for the underlying structure of  
194 slope information of EPIC-IIASA, from which the three highest slope classes (16–30 %, 30–45 %, >45 %) mark  
195 slopes that are less likely to be cultivated without measures to prevent erosion. We choose the MUSS equation  
196 for the baseline scenario as it generates the lowest deviation between simulated and measured water erosion as  
197 discussed below. Table 3 summarises the field management assumptions of the baseline scenario used to aggregate  
198 erosion rates in each grid cell and region.

### 199 **2.3 Uncertainty analysis of field management scenarios and water erosion equations**

200 Given the global scale of the analysis and the aggregated nature of available field management information, there  
201 is much uncertainty about crop management strategies, which introduces uncertainty in the water erosion  
202 estimates. In addition, each water erosion equation gives a different overall erosion estimate. To discuss the  
203 uncertainty of simulation results, we evaluate the variance in simulated water erosion rates at grid level due to: (i)  
204 different management assumptions, and (ii) the choice of water erosion equation. The variance of simulation  
205 outputs is defined as the range between minimum and maximum simulated water erosion rates with all  
206 combinations of tillage and cover crop scenarios and with each water erosion equation.

### 207 **2.4 Sensitivity analysis of model parameters**

208 We use a sensitivity analysis to identify the most essential input parameters to the factors in the seven water  
209 erosion equations. We use the Sobol method (Sobol, 1990), which is a variance-based sensitivity analysis that is  
210 popular in environmental modelling (Nossent et al., 2011). With this method, it is possible to quantify the amount  
211 of variance that each parameter contributes to the total variance of the model output. These amounts are expressed  
212 as sensitivity indices, which rank the importance of each input parameter for simulated water erosion. In addition,  
213 the sensitivity indices can be used to determine the impact of parameter interactions on the model output.

214 We test 30 parameters directly connected to the water erosion equations in EPIC. In total, we assign 126,976  
215 random values to all input parameters along a pre-defined triangular distribution or a range of discrete values  
216 (Table S2). Water erosion is simulated with EPIC using the seven available equations for each random input  
217 combination at 40 locations where wheat and maize are cultivated. To represent a heterogenous distribution of  
218 global precipitation regimes, we use the natural break optimisation method to choose locations based on average  
219 annual precipitation amounts from 1980 to 2010 (Jenks, 1967). For each location and equation, the most sensitive  
220 parameters are ranked. To analyse the impact of precipitation regimes on the sensitivity of each parameter, we use  
221 Spearman coefficients ( $\rho$ ) to determine if positive or negative relationships exist between each parameter's  
222 sensitivity and annual precipitation.

### 223 **2.4 Evaluation of simulated erosion against reported field measurements**

224 We compare our simulated water erosion rates with 606 soil erosion measurements on arable land from 36  
225 countries representing plot and field scale. Most of the selected erosion rates are based on the  $^{137}\text{Cs}$  method. In  
226 addition, data from erosion plots and volumetric measurements of rills collected by Auerwald et al. (2009),

227 Benaud et al. (2020) and García-Ruiz et al. (2015) are used. In total, 315 records are derived by the  $^{137}\text{Cs}$  method,  
228 188 records from runoff plots, and 103 records from volumetric measurements of rills. An overview of the field  
229 data is presented in Fig. S4-S7, and the full dataset is available in Table S5.

230 Guidance on the  $^{137}\text{Cs}$  method is provided by Fulajtar et al. (2017); Mabit et al. (2014) and Zapata (2002). The  
231  $^{137}\text{Cs}$  radionuclide was released by nuclear weapon tests and from the accident of the Chernobyl Nuclear Power  
232 Plant to the atmosphere and subsequently deposited in the uppermost soil layer by atmospheric fallout. After its  
233 deposition it was bind to soil colloids and can be moved only together with soil particles by mechanical processes  
234 such as soil erosion. Its chemical mobility and uptake by plants is negligible (Mabit et al., 2014; Zapata, 2002). If  
235 part of the topsoil contaminated by  $^{137}\text{Cs}$  is removed by erosion, the  $^{137}\text{Cs}$  concentrations in soil profiles can be  
236 used to trace soil movements using mass balance equation (Walling et al., 2014). A major advantage of the  $^{137}\text{Cs}$   
237 method is that it provides long term mean erosion rates (representing the period since  $^{137}\text{Cs}$  fallout in the 1960s  
238 until the time of sampling) and overcomes the problem of high temporal variability of erosion.

239 Bounded plots are the most commonly used method of erosion measurements. They were introduced in the USA  
240 in the 1920s (Hudson, 1993) and were used for the development of USLE and WEPP models (Brazier, 2004).  
241 Eroded soil material can be quantified with erosion plots in different ways (total collection of sediment, fractioned  
242 collection of sediments using multislot divisors, measurement of discharge and sediment concentration by tipping  
243 buckets and Coshocton wheels). The overview of this method is provided by Cerdan et al. (2010); Hudson (1993);  
244 Mutchler et al. (1994); De Ploey and Gabriels (1980) and Zachar (1982).

245 The volumetric measurements of rill erosion are used since approximately the 1940s in the USA (Kaiser, 1978 in  
246 Evans, 2013) and the 1950s in Europe (Lobotka, 1955), usually at field scale (Boardman, 1990, 2003; Boardman  
247 and Evans, 2020; Brazier, 2004; Evans, 2002, 2013; Herweg, 1988; Zachar, 1982). The volume of erosion rills is  
248 derived from their lengths and profile cross-section areas, which are measured in field or from terrestrial and aerial  
249 photos (Evans, 1986, 1988; Watson and Evans, 1991).

250 The overwhelming effect of the experimental methodology on measured erosion rates, the lack of sufficient  
251 metadata accompanying erosion measurements and the granular spatial resolution of our simulation setup hinders  
252 a direct comparison between simulated and observed water erosion rates. Instead we compare aggregated  
253 simulated and observed erosion values for different slope and precipitation classes to analyse the robustness of  
254 simulated water erosion rates under different environmental conditions. Therefore, only measurements with  
255 recorded slope steepness and annual precipitation are used. Where annual precipitation is not recorded, it is taken  
256 from the WorldClim2 dataset (Fick and Hijmans, 2017). Due to the non-normal distribution of the simulated and  
257 measured data, the median deviation (MD) is used as a measure to compare the agreement between simulated and  
258 measured water erosion values.

### 259 **3 Results**

260 We estimate global median water erosion rates of  $7 \text{ t ha}^{-1}$  and  $5 \text{ t ha}^{-1}$  in maize and wheat fields, respectively. The  
261 total removal of soil in global maize and wheat fields is estimated to be  $5.3 \text{ Gt a}^{-1}$  and  $1.9 \text{ Gt a}^{-1}$ , respectively. The  
262 map in Figure 2 illustrates the global distribution of simulated water erosion rates. Highest water erosion is  
263 simulated in mountainous regions and regions with strong precipitation, especially in tropical climate zones. In  
264 Asia, those regions are widespread in the east, south-east and the Himalaya region. In Africa, similar areas with

265 high water erosion values are spread around the continent and are most common at the west coast and in East  
266 Africa including broad areas in Guinea, Sierra Leone, Liberia, Ethiopia and Madagascar. In South America,  
267 highest water erosion is simulated in the south of Brazil and regions around the Andes mountain range and the  
268 Amazon river basin. The highest water erosion values on the American continent are simulated in tropical Central  
269 America and the Caribbean. In North America, highest water erosion occurs along the west coast and in the east.  
270 Water erosion in Europe is highest in Mediterranean areas and around the Alps.

271 Median annual water erosion values for the five largest wheat and maize producing countries demonstrate the  
272 strong impact of climate and topography on simulated water erosion. In Brazil, China and India, where a large  
273 proportion of cropland is in tropical areas, water erosion is relatively high with annual median values of 10 t ha<sup>-1</sup>,  
274 6 t ha<sup>-1</sup>, and 37 t ha<sup>-1</sup>, respectively. In Russia and the United States annual median values are much lower with 1 t  
275 ha<sup>-1</sup>, and 2 t ha<sup>-1</sup>, respectively. Overall, Figure 2 illustrates the large variation in simulated water erosion between  
276 tropical climate regions and regions with a large proportion of flat and dry land.

### 277 **3.1 Sources of model uncertainty related to management assumptions and method selection**

278 The uncertainty of the simulation results due to management scenarios and the choice of water erosion equations  
279 is highest in regions most vulnerable to water erosion (Figure 3). The annual median uncertainty range at each  
280 grid cell due to management is 30 t ha<sup>-1</sup>. For 97 % of grid cells, the lowest erosion rates are simulated with  
281 management scenarios including no-tillage and cover crops. For 86 % of grid cells, maximum erosion rates are  
282 simulated under conventional tillage without cover crops. The annual median uncertainty range at each grid cell  
283 due to the choice of erosion equation is 23 t ha<sup>-1</sup>. In 74 % of grid cells, the lowest erosion rates are simulated with  
284 the MUSS equation. The highest erosion values are simulated with the RUSLE equation (46 %), followed by the  
285 USLE equation (25%).

286 In most locations, the uncertainty due to field management exceeds the uncertainty caused by choice of erosion  
287 equation. For 46 % of grid cells, management scenarios cause the prevailing uncertainty, which we defined as the  
288 higher uncertainty range by at least 5 t ha<sup>-1</sup>. The selected erosion equation causes higher uncertainty by at least 5  
289 t ha<sup>-1</sup> in 14 % of grid cells. The map in Figure 4 illustrates the global distribution of prevailing uncertainty sources.

### 290 **3.2 Main drivers of the global erosion model**

291 We designed the sensitivity study to explain the large variability of simulated water erosion rates in different  
292 regions and to discuss the main differences between water erosion equations. Water erosion is highly sensitive to  
293 slope steepness (SLP) for all equations. The first-order sensitivity index of the slope parameter indicates that 46–  
294 54 % of the variance in the model output is attributable to the slope, without considering interactions between the  
295 input parameters (Table 4). Daily precipitation (PRCP) is the second most important parameter for calculating  
296 water erosion, with an individual contribution of around 9–20 % to the variance of the output. The remaining  
297 parameters contribute together 4–13 % to the output variance.

298 The first-order sensitivity indices do not include interactions between input parameters, which leads to the sum of  
299 all first-order sensitivity indices being lower than 1. The total-order sensitivity indices sum all first-order effects  
300 and interactions between parameters, which leads to overlaps in case of interactions and a sum greater than 1. The  
301 differences between the first-order and the total-order indices can be used as a measure to determine the impact  
302 of the interactions between a specific parameter with other parameters. The total-order sensitivity indices show

303 that slope steepness, including interactions to other parameters, contributes 63–75 % of the output variance from  
304 which 18–21 % are due to interactive effects with other parameters (Table 5). The total-order sensitivity indices  
305 from precipitation range from 21–36 %, from which 10–18 % is due to interactions with other parameters.

306 The high sensitivity of slope and precipitation is similar for all equations, but the most sensitive parameters after  
307 these can be different for each equation. Equations estimating erosion energy by surface runoff and the RUSLE2  
308 equation are very sensitive to the hydrological soil group (HSG), which determines the soils infiltration ability.  
309 This parameter is used in the calculation of the curve number, which defines the partition of precipitation into  
310 runoff and infiltration. Also, the land use number (LUN), which is ranked among the most sensitive input  
311 parameters, is used for the calculation of the curve number. The most sensitive parameters of the USLE and  
312 RUSLE equation, following slope inclination and daily precipitation, are soil texture classes (SAND & SILT)  
313 followed by daily temperature changes (TMX). Crop residues (ORHI) are relatively important for all equations  
314 but especially important for equations based on rainfall-energy. Other parameters relevant for field management,  
315 such as surface roughness and mixing efficiency of the topsoil, have little influence on water erosion.

316 The sensitivity of slope steepness has a strong positive correlation with the amount of annual precipitation at each  
317 location ( $\rho = 0.69$ ,  $p < 0.01$ ). The increase in the sensitivity of slope steepness with increasing annual precipitation  
318 is demonstrated in Figure 5, which illustrates substantially lower sensitivity indices at dry locations compared to  
319 wet locations. In contrast, the sensitivity indices of daily precipitation are negatively correlated to annual  
320 precipitation with a moderate strength ( $\rho = 0.45$ ,  $p < 0.05$ ). Depending on the equation, strong positive or negative  
321 correlations between SIs and annual precipitation also exist for other parameters such as slope length, soil texture,  
322 soil organic carbon, channel length, channel slope and watershed area (Table S4).

### 323 **3.3 Evaluation of simulation results against field data**

324 The most recent estimated global water erosion rates on cropland of 11 - 13 t ha<sup>-1</sup> derived from a comparable  
325 method (Borrelli et al., 2017; Doetterl et al., 2012; van Oost et al., 2007) lie above our simulated median water  
326 erosion rates of 7 t ha<sup>-1</sup> and 5 t ha<sup>-1</sup> for maize and wheat fields, respectively. Similarly, our global water erosion  
327 estimates in maize and wheat fields are lower than the median value of 9 t ha<sup>-1</sup> from 606 water erosion  
328 measurements from cropland around the world.

329 To evaluate the agreement between simulated and observed data, we compare median values between simulated  
330 and measured erosion rates grouped by precipitation and slope classes, which are defined along the whole range  
331 of recorded slope inclinations and annual precipitation amounts of the field data (Figure 6a). Although slope and  
332 precipitation classes from the field are spread unevenly, they cover most climatic and topographic characteristics  
333 relevant to global agriculture. The comparison illustrates that the deviation between simulated and field data is  
334 highest for locations with steep slopes and high annual precipitation. Where slopes are steeper than 8 % and annual  
335 precipitation is higher than 1000 mm, the median of simulated water erosion exceeds the median of measured  
336 water erosion in most cases by at least 50 t ha<sup>-1</sup>. With decreasing slope steepness and annual precipitation, the  
337 median deviation between simulated and measured data is decreasing. Where both slope steepness is below 8 %  
338 and annual precipitation is below 1000 mm, the median deviation is lower than 5 t ha<sup>-1</sup> in most cases. A comparison  
339 of measured and simulated water erosion using other equations with the baseline scenario can be found in Fig. S8.

340 The boxplots in Figure 6b illustrate the range of water erosion values measured in the field and simulated with the  
341 baseline scenario. The high deviation between observed and simulated values for grouped locations with slopes  
342 steeper than 8 % and annual precipitation higher than 1000 mm can also be observed between the range of  
343 simulated and measured water erosion values. Outside locations combining steep slopes and strong precipitation,  
344 median deviation between simulated and measured data is lower than the variability within the field data. The  
345 range of values at locations with lower precipitation and slope steepness demonstrates that simulated values are  
346 mostly below measured values in those environments.

347 The uncertainty in the choice of management scenarios and water erosion equations included in our baseline  
348 scenario leads to an uncertainty of the deviation between simulated and measured erosion values. This uncertainty  
349 is demonstrated in Figure 6b by additional three bars illustrating the range of simulated medians due to contrasting  
350 tillage management scenarios, cover crop scenarios and different water erosion equations. At locations with low  
351 to moderate slope steepness and annual precipitation, the measured water erosion values agree best with the  
352 simulation values generated under scenarios implying larger water erosion, such as high intensity tillage and low  
353 soil cover. On the other hand, at locations with steep slopes and intensive precipitation, the measured values are  
354 closer to the simulated values under scenarios with less intensive tillage and more soil cover. In addition, the  
355 varying sensitivities of each water erosion equation lead to a different magnitude of water erosion values in  
356 different environments. On low to moderate slopes, water erosion simulated with the MUSS equation is lowest,  
357 whereas RUSLE generates the highest values. On steep slopes, the RUSLE equation generates the lowest water  
358 erosion values, which agree best with the measured values. The options to increase and decrease simulated water  
359 erosion with different field management scenarios and water erosion equations creates both uncertainty in the  
360 model results, but also the possibility to closely match field data.

361 At locations combining steep slopes and intense precipitation, most management scenarios and equations generate  
362 water erosion values that are higher than the measured values. However, those environmental conditions cover  
363 only a small share of global cropland. Cultivation areas with slopes steeper than 8 % and annual precipitation  
364 higher than 1000 mm represent only 7 % of global maize and wheat cropland in our grid cells. The map in Figure  
365 7 illustrates that the highest concentration of these areas is in East and South-East Asia, followed by Central and  
366 South America, and Sub-Saharan Africa.

367

## 368 **4 Discussion**

### 369 **4.1 Varying robustness of simulated water erosion in different global regions**

370 Global water erosion estimates generated with an EPIC-based GGCM and our baseline scenario overlap with  
371 observed water erosion values under most of the climatic and topographic environments where maize and wheat  
372 are grown. However, global maize and wheat land include locations where environmental characteristics differ  
373 significantly from the Midwestern United States, where the data was collected to develop the water erosion  
374 equations embedded in EPIC. The USLE model and its modification were developed with data for slopes of up to  
375 20 %, which makes model application for steeper slopes uncertain (McCool et al., 1989; Meyer, 1984).  
376 Furthermore, the relations between kinetic energy and rainfall energy in the American Great Plains differ from  
377 other regions in the world (Roose, 1996). Similarly, the runoff curve number method, which is the key

378 methodology for the calculation of surface runoff, is based on an empirical analysis in watersheds located in the  
379 United States and might be less reliable in different regions of the world (Rallison, 1980). Due to the high  
380 sensitivity of slope steepness and daily precipitation for the calculation of water erosion, the reliability of the  
381 tested equations decreases in regions where typical slope and precipitation patterns differ from the Midwestern  
382 US. Although some studies have successfully used USLE and its modification under a different environmental  
383 context (e.g. Alewell et al., 2019; Almas and Jamal, 2009; Fischer et al., 2018; Sadeghi and Mizuyama, 2007),  
384 many studies have concluded that the accuracy of these models may be reduced outside the environments they  
385 were created without calibration and model adaptation (e.g. Cohen et al., 2005; Labrière et al., 2015).

386 The skewed distribution of simulated water erosion values influenced by extreme soil loss rates in few fields  
387 highly sensitive to water erosion results in a large difference between the global median value of  $6 \text{ t ha}^{-1} \text{ a}^{-1}$  and  
388 the global average value of  $19 \text{ t ha}^{-1} \text{ a}^{-1}$  (Fig. S9). Due to the strong influence of outliers on average values, we  
389 used median values to represent global and regional water erosion rates in wheat and maize fields. The high  
390 sensitivity of the simulation results to slope inclinations and precipitation suggests that a significant share of the  
391 estimated soil removal of  $7.2 \text{ Gt a}^{-1}$  originates from small wheat and maize cultivation areas on steep slopes with  
392 strong annual precipitation.

## 393 **4.2 Sources of uncertainties in global water erosion estimates**

### 394 **4.2.1 Uncertain land use in mountainous regions**

395 Changing climatic conditions with increasing elevation and the variable soils in mountainous regions can favour  
396 crop cultivation in higher elevations over lower elevations (Romeo et al., 2015). However, upland farming without  
397 soil conservation measures can lead to exhaustive soil erosion and can become a critical problem for agriculture  
398 (Montgomery, 2007). Large areas of land have been abandoned due to high erosion rates as soils were no longer  
399 able to support crops (Figure 8) (Romeo et al., 2015). As mountain agriculture is determined by various  
400 environmental and socio-economic factors, the cultivation of steep slopes can be very variable between regions.  
401 Regional erosion assessments in mountainous cropland suggested that areas with extreme water erosion rates are  
402 mainly limited to marginal steep land cultivated by smallholders (Haile and Fetene, 2012; Long et al., 2006;  
403 Nyssen et al., 2019). In some mountainous regions, efforts to remove marginal farmlands from agricultural  
404 production, and programs to improve land management on steep slopes have reduced high water erosion rates  
405 (Deng et al., 2012; Nyssen et al., 2015). On the contrary, recent pressure through increasing population and crop  
406 production demands has resulted in re-cultivation of hillslopes and a reduction of fallow periods, which limits the  
407 recovery of eroded soil (Turkelboom et al., 2008; Valentin et al., 2008).

408 To analyse the sustainability of simulated maize and wheat cultivation systems exposed to high erosion rates, we  
409 compare simulated annual eroded soil depth with a global dataset on modelled sedimentary deposit thickness  
410 (Pelletier et al., 2016). The comparison shows that at 4 % of grid cells permanent maize and wheat cultivation  
411 would not be sustainable as the whole soil profile would be eroded at the end of the simulation period (Fig.  
412 [S10S18](#)). Most of the unsustainable agriculture is simulated on steep slopes. Although we account for conservation  
413 techniques and cover crops, we do not imitate the highly complex farming practices involving intercropping  
414 techniques and fallow periods, which are common on hillslopes typically managed by smallholders (Turkelboom  
415 et al., 2008). Moreover, we assume that the slope class representing the largest area in each grid cell most likely  
416 represents the largest share of arable land. This builds on the idea that a spatially extensive and diverse landscape

417 can be represented by a single “representative field” characterized by the prevailing topography and soil conditions  
418 found in the landscape. On hilly terrain this setup simulates maize and wheat cultivation on steep slopes and thus  
419 mainly represents unsustainable agriculture. Although unsustainable maize and wheat cultivation can be observed  
420 in several mountain regions, cropland is very heterogeneously distributed in mountains and thus erosion rates  
421 from one representative field are highly uncertain.

422 The uncertainty in cropland distribution can partly be reduced by developing a higher resolution global gridded  
423 data infrastructure, which is currently not available for EPIC-IIASA. However, due to the large uncertainty in  
424 global land cover maps (Fritz et al., 2015; Lesiv et al., 2019), an explicit spatial link between cropland distribution  
425 and the corresponding slope category cannot be established without on-site observations. We test the impact of  
426 this uncertainty for erosion estimates in Italy, where large maize and wheat cultivation areas are distributed on  
427 both flat terrain in the north and mountainous regions in the south. In an ideal scenario where cropland is limited  
428 to flattest land available per grid cell, median simulated water erosion in Italy would be reduced to tolerable levels  
429 below  $1 \text{ t ha}^{-1}$ . However, in a scenario, where the most common slopes per grid cell are cultivated, median  
430 simulated water erosion increases to  $14 \text{ t ha}^{-1}$  due to high water erosion simulated in Italy’s mountainous regions  
431 (Fig. S4+S19). This suggests a high uncertainty in global water erosion estimates due to uncertain spatial links  
432 between maize and wheat cultivation areas and different slope categories.

#### 433 **4.2.2 Uncertain field management**

434 Simulated water erosion values are highly variable depending on the field management scenario. Simulating cover  
435 crop and no-tillage worldwide results in the lowest global soil removal of  $2 \text{ Gt a}^{-1}$  with median water erosion rates  
436 of  $1 \text{ t ha}^{-1} \text{ a}^{-1}$  and simulating no cover crops and conventional tillage worldwide results in the highest global soil  
437 removal of  $13 \text{ Gt a}^{-1}$  with median water erosion rates of  $17 \text{ t ha}^{-1} \text{ a}^{-1}$ . These variations cause further uncertainties  
438 in the simulation results.

439 Indeed, a proper reconstruction of a business-as-usual field management is important to further narrow down the  
440 uncertainty in global crop modelling (Folberth et al., 2019). In this study we allocated prevailing field management  
441 using a set of environmental- and country-specific indicators, similarly to Porwollik et al. (2019). For example,  
442 we accounted for conservation agriculture only in countries where this management strategy is likely according  
443 to AQUASTAT (FAO, 2016). Furthermore, by assuming cover crops in between wheat and maize seasons we  
444 simulated more complex cropping systems in the tropics, where long and year-round growing seasons and frequent  
445 multi-cropping farm practices barely leave the soil uncovered. Hence, we did not simulate bare fallow in the  
446 tropics as erroneously high water erosion values would have been simulated at locations with heavy precipitation  
447 falling on bare soil. In addition, conservation practices such as contouring and terracing are crucial to reduce the  
448 simulation of high water erosion values on steep slopes. We simulated these practices for specific slope classes  
449 under the assumption that farmers around the world uniformly use conservation practices when cultivating on  
450 steep slopes. The most relevant parameters used for tillage scenarios are related to crop residues left in the field.  
451 In addition, equations directly connected to surface runoff are strongly influenced by the land use number used to  
452 determine the impact of cover type and treatment on soil permeability. While both crop residues and green fallow  
453 decrease water erosion significantly, especially in the tropics, their use varies widely between regions and even  
454 farms, based on a complex web of factors such as institutional factors, farm sizes, risk attitudes, interest rates,  
455 access to markets, farming systems, resource endowments, and farm management skills (Pannell et al., 2014).

456 Also, soil conservation measures such as terraces or contour farming significantly influence water erosion but are  
457 very heterogeneously used between regions, farming systems and farmers. Our baseline scenario is a very rough  
458 depiction of the complex patterns of field management around the world but attempts to represent these highly  
459 influential practices with the limited available data.

#### 460 **4.2.3 Variable estimates from different water erosion equations**

461 The water erosion equation chosen for the baseline scenario generates the lowest global soil removal estimate.  
462 Different water erosion equations embedded in EPIC estimate a higher global soil removal of up to 11 Gt a<sup>-1</sup> as  
463 well as higher median water erosion rates up to 19 t ha<sup>-1</sup> a<sup>-1</sup>. The MUSS water erosion equation chosen for the  
464 baseline scenario generates water erosion rates closest to the field data. The focus of equations on either rainfall  
465 energy or runoff energy is relevant for the different simulation results under specific environmental conditions.  
466 Equations based on rainfall-energy such as RUSLE and USLE simulate higher water erosion values than the other  
467 equations at most locations. However, on steep slopes they generate the lowest water erosion values as runoff  
468 becomes a greater source of energy than rain with increasing slope steepness (Roose, 1996). Also, the varying  
469 sensitivities of other parameters to the equations such as soil properties and management parameters lead to a  
470 varying agreement between simulated data and field data depending on the equation selection. Detailed field data  
471 would facilitate the choice of an appropriate equation to simulate water erosion worldwide or for a specific region.

#### 472 **4.3 The difficulty of evaluating large-scale erosion estimates with field data**

473 The selection of field data for evaluating simulated water erosion was limited by the low availability of suitable  
474 water erosion observations covering the entire globe. The lack of reliable data on water erosion rates is a severe  
475 obstacle for understanding erosion, developing and validating models and implementing soil conservation  
476 (Boardman, 2006; Nearing et al., 2000; Poesen et al., 2003; Trimble and Crosson, 2000). The main reasons for  
477 the low availability of suitable data to evaluate simulated water erosion rates are twofold: (i) erosion monitoring  
478 is expensive, time consuming and labour demanding; and, (ii) primary data and metadata of measurement sites  
479 accompanying final results are often not available and many older measurements are poorly accessible as they are  
480 not available online (Benaud et al., 2020). A variety of factors influencing water erosion such as climate, field  
481 topography, soil properties and field management need to be considered when modelling water erosion but are  
482 often not reported in available field measurements (García-Ruiz et al., 2015). This hampers a direct comparison  
483 between simulated and observed water erosion values. We demonstrated the varying match between measured  
484 and simulated water erosion using different tillage and cover crop scenarios. Metadata on field management often  
485 only provides the crop cultivated and therefore the conditions under which erosion was measured in the field are  
486 not known sufficiently to evaluate erosion values simulated under different field management scenarios. Similarly,  
487 information on field topography and soil properties is often not provided with recorded field measurements and  
488 thus their use is limited in an evaluation of water erosion estimates simulated in different global environments.  
489 Moreover, most data are concentrated in the United States, West Europe and the West Mediterranean (García-  
490 Ruiz et al., 2015). In summary, there is a lack of field data representing all needed regions, situations and scenarios  
491 (Alewell et al., 2019).

492 The appropriate selection of field data to evaluate model outputs needs to be considered as well. At different  
493 spatial scales different erosion processes are dominant and consequently different erosion measurement methods  
494 are suitable (Boix-Fayos et al., 2006; Stroosnijder, 2005). Most authors use very heterogeneous data sets to



495 evaluate their models, involving data generated by different methods at variable time and spatial scales and  
496 variable quality. For example, Doetterl et al. (2012) used plot data, suspended sediments from rivers, and data  
497 from RUSLE modelling. Borrelli et al. (2017) used soil erosion rates (measurement methods are not specified),  
498 remote sensing, vegetation index (NDVI) and results of RUSLE modelling. In his review on erosion rates under  
499 different land use, Montgomery (2007) used field data derived from erosion plots, field-scale measurements,  
500 catchment-scale measurements using hydrological methods, <sup>137</sup>Cs-method, soil profile truncation and elevated  
501 cemetery plots.

502 Whilst all erosion measurement methods are open to criticism, we decided to use only data obtained by field  
503 measurements from runoff plots, by <sup>137</sup>Cs method and volumetric surveys as these methods are most suitable at  
504 plot, slope and field scale. Geodetic methods such as erosion pins and laser scanner are also used at plot to field  
505 scales, but their accuracy is much lower than the accuracy of plot measurements and <sup>137</sup>Cs method. Furthermore,  
506 erosion pins are mainly suitable for areas with extreme erosion rates (Hsieh et al., 2009; Hudson, 1993), and laser  
507 scanners have difficulties to recognize vegetation (Hsieh et al., 2009). Other commonly used methods such as  
508 hydrological method (measurements of discharge and suspended sediment load) and bathymetric method are more  
509 suitable for larger scales and involve a significant portion of channel erosion, which is not related with agricultural  
510 land (García-Ruiz et al., 2015). We did not consider plot experiments using rainfall simulators as they are usually  
511 performed on small plots with artificially generated rainfalls, which mostly have very low energies and thus  
512 generate low erosion rates (Boix-Fayos et al., 2006; García-Ruiz et al., 2015).

513 The <sup>137</sup>Cs method was criticised by Parsons and Foster (2013), who questioned assumptions about the <sup>137</sup>Cs  
514 behaviour in the environment (variability of the <sup>137</sup>Cs input by wet fallout, its microspatial variability at reference  
515 sites, its possible mobility in certain soils, the <sup>137</sup>Cs uptake by plants and other aspects of <sup>137</sup>Cs behaviour in soil).  
516 To confront the criticism against the <sup>137</sup>Cs method, Mabit et al. (2013) discussed all objections raised by Parsons  
517 and Foster (2013) and confirmed its accuracy by listing several studies, in which <sup>137</sup>Cs based erosion rates are  
518 compared with erosion rates derived from direct measurements. The <sup>137</sup>Cs method is based on a set of  
519 presumptions which should be met to produce useful results and thus careful interpretation of the obtained results  
520 is needed (Fulajtar et al., 2017; Mabit et al., 2014; Zapata, 2002).

521 Similarly, erosion rates obtained by volumetric measurements require careful interpretation as they are exposed  
522 to various potential sources of errors and do not account for interill erosion. Although the latter can be neglected  
523 under certain circumstances, studies from Europe and semiarid areas of the USA have reported that interill erosion  
524 contributed significantly to the amount of soil eroded in fields (Boardman and Evans, 2020; Parsons, 2019).  
525 Further, measuring the lengths and cross-sections of rills during field surveys or on terrestrial and aerial photos  
526 can be very subjective (Panagos et al., 2016). Different approaches used to detect and measure rills in fields can  
527 cause variability in calculated erosion volumes up to a factor of two (Boardman and Evans, 2020; Casali et al.,  
528 2006; Watson and Evans, 1991). In order to obtain soil erosion rates in weight units, soil volumes need to be  
529 converted using the soil bulk density, which is often based on estimates (Evans and Brazier, 2005).

530 The shortcomings of erosion plot measurements were discussed by several authors (Auerswald et al., 2009;  
531 Brazier, 2004; Evans, 1995, 2002; Loughran et al., 1988). Erosion plots have various sizes and shapes (few meters  
532 to few hundreds of meters) and various approaches of sediment recording are used (total collection, multislots

533 divisors, tipping buckets, Coshocton wheels), which all involve significant uncertainties. Although some long-  
534 term plot experiments exist, many plot measurements fail to cover the whole year erosion cycle (Auerswald et al.,  
535 2009). Often, they have to be removed during land management operations such as seeding, ploughing, or they  
536 are too expensive and labour demanding.

537 Despite all the shortcomings of available soil erosion data, most data provide valuable information (Benaud et al.,  
538 2020). The evaluation against field measurements in this study provided a first indication of the robustness of  
539 results under specific topographic and climatic conditions. In most environments relevant for maize and wheat  
540 cultivation the deviation between simulated and measured water erosion values is lower than the variability within  
541 the field data. The reported data does not enable us to further narrow down the uncertainties addressed. Although  
542 the metadata accompanying the field measurements includes information on slope steepness and annual  
543 precipitation (or geographic coordinates allowing for overlay with climatic data), information on soil types or  
544 texture classes, crop type and tillage system implemented over time are provided only for few points. Also, the  
545 various methods used to measure erosion rates, their complex implementation and the bias of field studies towards  
546 locations sensitive to erosion lead to an uncertain representation of large-scale erosion rates based on field  
547 measurements. To facilitate in-depth evaluation of erosion models across different scales, it is crucial to provide  
548 detailed information on site characteristics and to harmonise approaches to measure erosion in the field. Moreover,  
549 the accessibility of field data should be improved as raw data is often not published or needs to be collected from  
550 numerous publications, grey literature and conference proceedings to obtain the large amount of data necessary  
551 for regional or global erosion studies. Therefore, we support recent efforts to collate erosion measurements and  
552 metadata from existing studies (Benaud et al., 2020) as we believe that the availability of field data through a  
553 single platform will greatly benefit future modelling studies and the understanding of soil erosion at all scales.

554

## 555 **5 Conclusion**

556 The simulation of water erosion with GGCMs is largely influenced by the resolution of global datasets providing  
557 topographic, soil, climate, land use and field management data, which is currently not available at the field scale.  
558 Yet, considering water erosion in global crop yield projections can provide useful outputs to inform assessments  
559 of the potential impacts of erosion on global food production and to identify soil erosion hotspots on cropland for  
560 management and policy interventions. To improve the quality of the estimates and to further develop these models,  
561 it is crucial to identify, communicate and address the existing uncertainties. Increasing the resolution of global  
562 soil, topographic and precipitation data is central for improving global water erosion estimates. In addition, this  
563 study provides an insight into the importance of considering field management. The numerous options to simulate  
564 the cultivation of fields result in a large range of possible water erosion values, which can only partly be narrowed  
565 down at a global scale. Further improvement of global water erosion estimates requires detailed and harmonized  
566 field measurements across all environmental conditions to validate and calibrate simulation outputs. Using  
567 existing field data, we were able to identify specific environmental characteristics for which we have lower  
568 confidence in the modelled erosion rates. These are mainly found in the tropics and mountainous regions due to  
569 the high sensitivity of simulated water erosion to slope steepness and precipitation strength, and the complexity  
570 of mountain agriculture. However, these areas represent only a small fraction of global cropland for maize and  
571 wheat. The overlap of simulated and measured water erosion values in most environments used to produce maize

572 and wheat underlines the robustness of an EPIC-based GGCM to simulate the differences in water erosion rates  
573 of major global crop production regions.

574 **Data availability.** Additional information on model outputs, methods, study design and field data are available  
575 in the supporting information file: TWCarr-si.zip.

576 **Author contributions.** TC, JB, CF and RS designed the study. TC, JB, CF, EF and RS collected and analysed  
577 the data. TC prepared the manuscript with contributions from all co-authors.

578 **Competing interests.** The authors declare that they have no conflict of interest.

579 **Acknowledgement.** This project has received funding from the Grantham Foundation and the European Union's  
580 Horizon 2020 research and innovation programme under grant agreement No 776810 (VERIFY) and No 774378  
581 (CIRCASA). We would like to thank three anonymous reviewers for their help to improve this paper.

582

## 583 **References**

584 Alewell, C., Borrelli, P., Meusburger, K. and Panagos, P.: Using the USLE: Chances, challenges and limitations  
585 of soil erosion modelling, *Int. Soil Water Conserv. Res.*, 7(3), 203–225, doi:10.1016/j.iswcr.2019.05.004, 2019.

586 Almas, M. and Jamal, T.: Use of RUSLE for Soil Loss Prediction During Different Growth Periods, *Pakistan J.*  
587 *Biol. Sci.*, 3(1), 118–121, doi:10.3923/pjbs.2000.118.121, 2009.

588 Auerswald, K., Kainz, M. and Fiener, P.: Soil erosion potential of organic versus conventional farming  
589 evaluated by USLE modelling of cropping statistics for agricultural districts in Bavaria, *Soil Use Manag.*, 19(4),  
590 305–311, doi:10.1079/sum2003212, 2004.

591 Auerswald, K., Fiener, P. and Dikau, R.: Rates of sheet and rill erosion in Germany - A meta-analysis,  
592 *Geomorphology*, 111(3–4), 182–193, doi:10.1016/j.geomorph.2009.04.018, 2009.

593 Balkovič, J., van der Velde, M., Skalský, R., Xiong, W., Folberth, C., Khabarov, N., Smirnov, A., Mueller, N.  
594 D. and Obersteiner, M.: Global wheat production potentials and management flexibility under the representative  
595 concentration pathways, *Glob. Planet. Change*, 122, 107–121, doi:10.1016/j.gloplacha.2014.08.010, 2014.

596 Balkovič, J., Skalský, R., Folberth, C., Khabarov, N., Schmid, E., Madaras, M., Obersteiner, M. and van der  
597 Velde, M.: Impacts and Uncertainties of +2°C of Climate Change and Soil Degradation on European Crop  
598 Calorie Supply, *Earth's Futur.*, 6(3), 373–395, doi:10.1002/2017EF000629, 2018.

599 Benaud, P., Anderson, K., Evans, M., Farrow, L., Glendell, M., James, M., Quine, T., Quinton, J., Rawlins, B.,  
600 Rickson, J. and Brazier, R.: National-scale geodata describe widespread accelerated soil erosion., *Geoderma*,  
601 371(April), 114378, doi:10.1016/j.geoderma.2020.114378, 2020.

602 Den Biggelaar, C., Lal, R., Wiebe, K., Eswaran, H., Breneman, V. and Reich, P.: The Global Impact Of Soil  
603 Erosion On Productivity\*. II: Effects On Crop Yields And Production Over Time, *Adv. Agron.*, 81(03), 49–95,  
604 doi:10.1016/S0065-2113(03)81002-7, 2004.

605 Boardman, J.: Soil erosion on the South Downs: a review, in *Soil Erosion on Agricultural Land*, edited by J.  
606 Boardman, I. D. L. Foster, and J. A. Dearing, pp. 87–105, John Wiley & Sons Ltd, Chichester., 1990.

607 Boardman, J.: Soil erosion and flooding on the eastern South Downs, southern England, 1976-2001, *Trans. Inst.*  
608 *Br. Geogr.*, 28(2), 176–196, doi:10.1111/1475-5661.00086, 2003.

609 Boardman, J.: Soil erosion science: Reflections on the limitations of current approaches, *Catena*, 68(2–3), 73–  
610 86, doi:10.1016/j.catena.2006.03.007, 2006.

611 Boardman, J. and Evans, R.: The measurement, estimation and monitoring of soil erosion by runoff at the field  
612 scale: Challenges and possibilities with particular reference to Britain, *Prog. Phys. Geogr.*, 44(1), 31–49,  
613 doi:10.1177/0309133319861833, 2020.

- 614 Boix-Fayos, C., Martínez-Mena, M., Arnau-Rosalén, E., Calvo-Cases, A., Castillo, V. and Albaladejo, J.:  
 615 Measuring soil erosion by field plots: Understanding the sources of variation, *Earth-Science Rev.*, 78(3–4), 267–  
 616 285, doi:10.1016/j.earscirev.2006.05.005, 2006.
- 617 Borrelli, P., Robinson, D. A., Fleischer, L. R., Lugato, E., Ballabio, C., Alewell, C., Meusburger, K., Modugno,  
 618 S., Schütt, B., Ferro, V., Bagarello, V., Oost, K. Van, Montanarella, L. and Panagos, P.: An assessment of the  
 619 global impact of 21st century land use change on soil erosion, *Nat. Commun.*, doi:10.1038/s41467-017-02142-  
 620 7, 2017.
- 621 Brazier, R.: Quantifying soil erosion by water in the UK: A review of monitoring and modelling approaches,  
 622 *Prog. Phys. Geogr.*, 28(3), 340–365, doi:10.1191/0309133304pp415ra, 2004.
- 623 Casali, J., Loizu, J., Campo, M. A., De Santisteban, L. M. and Alvarez-Mozos, J.: Accuracy of methods for field  
 624 assessment of rill and ephemeral gully erosion, *Catena*, 67, 128–138, 2006.
- 625 Cerdan, O., Govers, G., Le Bissonnais, Y., Van Oost, K., Poesen, J., Saby, N., Gobin, A., Vacca, A., Quinton,  
 626 J., Auerswald, K., Klik, A., Kwaad, F. J. P. M., Raclot, D., Ionita, I., Rejman, J., Rousseva, S., Muxart, T.,  
 627 Roxo, M. J. and Dostal, T.: Rates and spatial variations of soil erosion in Europe: A study based on erosion plot  
 628 data, *Geomorphology*, 122(1–2), 167–177, doi:10.1016/j.geomorph.2010.06.011, 2010.
- 629 CGIAR-CSI: NASA Shuttle Radar Topographic Mission (SRTM). The SRTM data is available as 3 arc second  
 630 (approx. 90m resolution) DEMs. The dataset is available for download at: <http://srtm.csi.cgiar.org/>, 2006.
- 631 Chappell, A., Baldock, J. and Sanderman, J.: The global significance of omitting soil erosion from soil organic  
 632 carbon cycling schemes, *Nat. Clim. Chang.*, 6(2), 187–191, doi:10.1038/nclimate2829, 2016.
- 633 Chung, S. W., Gassman, P. W., Kramer, L. A., Williams, J. R., Gu, R. R., Chung, S. W. ; Gassman, P. W. ;  
 634 Kramer, L. A. ; and Williams, J. R. ; Validation of EPIC for Two Watersheds in Southwest Iowa Recommended  
 635 Citation Validation of EPIC for Two Watersheds in Southwest Iowa, 1999.
- 636 Cohen, M. J., Shepherd, K. D. and Walsh, M. G.: Empirical reformulation of the universal soil loss equation for  
 637 erosion risk assessment in a tropical watershed, *Geoderma*, 124(3–4), 235–252,  
 638 doi:10.1016/j.geoderma.2004.05.003, 2005.
- 639 Deng, L., Shangguan, Z. ping and Li, R.: Effects of the grain-for-green program on soil erosion in China, *Int. J.*  
 640 *Sediment Res.*, 27(1), 120–127, doi:10.1016/S1001-6279(12)60021-3, 2012.
- 641 Doetterl, S., Van Oost, K. and Six, J.: Towards constraining the magnitude of global agricultural sediment and  
 642 soil organic carbon fluxes, *Earth Surf. Process. Landforms*, 37(6), 642–655, doi:10.1002/esp.3198, 2012.
- 643 Evans, R.: Finding out about water erosion, *Teach. Geogr.*, 12, 17–20, 1986.
- 644 Evans, R.: Water Erosion in England and Wales 1982–1984. Report for Soil Survey and Land Research Centre,  
 645 Silsoe., 1988.
- 646 Evans, R.: Some methods of directly assessing water erosion of cultivated land – a comparison of measurements  
 647 made in plots and in fields, *Prog. Phys. Geogr.*, 19, 115–129, 1995.
- 648 Evans, R.: An alternative way to assess water erosion of cultivated land – field-based measurements: An  
 649 analysis of some results, *Appl. Geogr.*, 22, 187–208, 2002.
- 650 Evans, R.: Assessment and monitoring of accelerated water erosion of cultivated land - when will reality be  
 651 acknowledged?, *Soil Use Manag.*, 29(1), 105–118, doi:10.1111/sum.12010, 2013.
- 652 Evans, R. and Boardman, J.: The new assessment of soil loss by water erosion in Europe. Panagos P. et al., 2015  
 653 *Environmental Science & Policy* 54, 438-447-A response, *Environ. Sci. Policy*, 58, 11–15,  
 654 doi:10.1016/j.envsci.2015.12.013, 2016.
- 655 Evans, R. and Brazier, R.: Evaluation of modelled spatially distributed predictions of soil erosion by water  
 656 versus field-based assessments, *Environ. Sci. Pol.*, 8, 493–501, 2005.
- 657 FAO/IIASA/ISRIC/ISSCAS/JRC: Harmonized World Soil Database (version 1.1), 2009.
- 658 FAO: AQUASTAT Main Database, [online] Available from:  
 659 <http://www.fao.org/nr/water/aquastat/data/query/index.html?lang=en> (Accessed 1 July 2020), 2016.

- 660 Fick, S. E. and Hijmans, R. .: Worldclim 2: New 1-km spatial resolution climate surfaces for global land areas,  
661 *Int. J. Climatol.*, 2017.
- 662 Fischer, F. K., Kistler, M., Brandhuber, R., Maier, H., Treisch, M. and Auerswald, K.: Validation of official  
663 erosion modelling based on high-resolution radar rain data by aerial photo erosion classification, *Earth Surf.*  
664 *Process. Landforms*, 43(1), 187–194, doi:10.1002/esp.4216, 2018.
- 665 Fisher, G., Nachtergaele, F., Prieler, S., van Velthuizen, H. T., Verelst, L. and Wiberg, D.: Global Agro-  
666 ecological Zones Assessment for Agriculture (GAEZ 2007), IIASA, Laxenburg, Austria and FAO, Rome, Italy.,  
667 2007.
- 668 Folberth, C., Elliott, J., Müller, C., Balkovič, J., Chryssanthacopoulos, J., Izaurralde, R. C., Jones, C. D.,  
669 Khabarov, N., Liu, W., Reddy, A., Schmid, E., Skalský, R., Yang, H., Arneth, A., Ciais, P., Deryng, D.,  
670 Lawrence, P. J., Olin, S., Pugh, T. A. M., Ruane, A. C. and Wang, X.: Parameterization-induced uncertainties  
671 and impacts of crop management harmonization in a global gridded crop model ensemble, *PLoS One*, 14(9),  
672 e0221862, doi:10.1371/journal.pone.0221862, 2019.
- 673 Fritz, S., See, L., McCallum, I., You, L., Bun, A., Moltchanova, E., Duerauer, M., Albrecht, F., Schill, C.,  
674 Perger, C., Havlik, P., Mosnier, A., Thornton, P., Wood-Sichra, U., Herrero, M., Becker-Reshef, I., Justice, C.,  
675 Hansen, M., Gong, P., Abdel Aziz, S., Cipriani, A., Cumani, R., Cecchi, G., Conchedda, G., Ferreira, S.,  
676 Gomez, A., Haffani, M., Kayitakire, F., Malanding, J., Mueller, R., Newby, T., Nonguierma, A., Olusegun, A.,  
677 Ortner, S., Rajak, D. R., Rocha, J., Schepaschenko, D., Schepaschenko, M., Terekhov, A., Tiangwa, A.,  
678 Vancutsem, C., Vintrou, E., Wenbin, W., van der Velde, M., Dunwoody, A., Kraxner, F. and Obersteiner, M.:  
679 Mapping global cropland and field size, *Glob. Chang. Biol.*, 21(5), 1980–1992, doi:10.1111/gcb.12838, 2015.
- 680 Fu, B. J., Zhao, W. W., Chen, L. D., Zhang, Q. J., Lü, Y. H., Gulinck, H. and Poesen, J.: Assessment of soil  
681 erosion at large watershed scale using RUSLE and GIS: A case study in the Loess Plateau of China, *L. Degrad.*  
682 *Dev.*, 16(1), 73–85, doi:10.1002/ldr.646, 2005.
- 683 Fulajtar, E., Mabit, L., Renschler, C. S. and Lee Zhi Yi, A.: Use of 137Cs for soil erosion assessment, FAO,  
684 Rome., 2017.
- 685 García-Ruiz, J. M., Beguería, S., Nadal-Romero, E., González-Hidalgo, J. C., Lana-Renault, N. and Sanjuán, Y.:  
686 A meta-analysis of soil erosion rates across the world, *Geomorphology*, 239, 160–173,  
687 doi:10.1016/j.geomorph.2015.03.008, 2015.
- 688 Haile, G. W. and Fetene, M.: Assessment of soil erosion hazard in kilie catchment, East Shoa, Ethiopia, L.  
689 *Degrad. Dev.*, 23(3), 293–306, doi:10.1002/ldr.1082, 2012.
- 690 Herweg, K.: The applicability of large-scale geomorphological mapping to erosion control and soil conservation  
691 in a research area in Tuscany, *Zeitschrift fur Geomorphol. Suppl.*, 68, 175–187, 1988.
- 692 Hsieh, Y. P., Grant, K. T. and Bugna, G. C.: A field method for soil erosion measurements in agricultural and  
693 natural lands, *J. Soil Water Conserv.*, 64(6), 374–382, doi:10.2489/jswc.64.6.374, 2009.
- 694 Hudson, N. W.: Field measurement of soil erosion and runoff, Food and Agriculture Organization of the United  
695 Nations. [online] Available from: <https://books.google.co.uk/books?id=rS1fiFU3rOwC>, 1993.
- 696 IIASA/FAO: Global Agro-ecological Zones (GAEZ v3.0), IIASA, Laxenburg, Austria and FAO, Rome, Italy.,  
697 2012.
- 698 Izaurralde, R. C., Williams, J. R., McGill, W. B., Rosenberg, N. J. and Jakas, M. C. Q.: Simulating soil C  
699 dynamics with EPIC: Model description and testing against long-term data, *Ecol. Modell.*, 192(3–4), 362–384,  
700 doi:10.1016/j.ecolmodel.2005.07.010, 2006.
- 701 Jenks, G. F.: The Data Model Concept in Statistical Mapping, *Int. Yearb. Cartogr.*, 7, 186–190, 1967.
- 702 Kaiser, J.: Wounding Earth ' s Fragile Skin, *Science* (80-. ), 304(June), 1616–1618,  
703 doi:10.1126/science.304.5677.1616, 2004.
- 704 Kaiser, V. G.: Annual erosion survey of Whitman county, Washington. 1939/40-1975/76, Spokane, WA 99201.,  
705 1978.
- 706 Karydas, C. G., Sekuloska, T. and Silleos, G. N.: Quantification and site-specification of the support practice  
707 factor when mapping soil erosion risk associated with olive plantations in the Mediterranean island of Crete,

- 708 Environ. Monit. Assess., 149(1–4), 19–28, doi:10.1007/s10661-008-0179-8, 2009.
- 709 Kottek, M., Grieser, J., Beck, C., Rudolf, B. and Rubel, F.: World Map of the Köppen–Geiger climate  
710 classification updated, Meteorol. Zeitschrift, 15(3), 259–263, doi:10.1097/00041433-200208000-00008, 2006.
- 711 Labrière, N., Locatelli, B., Laumonier, Y., Freycon, V. and Bernoux, M.: Soil erosion in the humid tropics: A  
712 systematic quantitative review, Agric. Ecosyst. Environ., 203, 127–139, doi:10.1016/j.agee.2015.01.027, 2015.
- 713 Lesiv, M., Laso Bayas, J. C., See, L., Duerauer, M., Dahlia, D., Durando, N., Hazarika, R., Kumar Sahariah, P.,  
714 Vakolyuk, M., Blyshchik, V., Bilous, A., Perez-Hoyos, A., Gengler, S., Prestele, R., Bilous, S., Akhtar, I. ul H.,  
715 Singha, K., Choudhury, S. B., Chetri, T., Malek, Ž., Bungnamei, K., Saikia, A., Sahariah, D., Narzary, W.,  
716 Danylo, O., Sturn, T., Karner, M., McCallum, I., Schepaschenko, D., Moltchanova, E., Fraisl, D., Moorthy, I.  
717 and Fritz, S.: Estimating the global distribution of field size using crowdsourcing, Glob. Chang. Biol., 25(1),  
718 174–186, doi:10.1111/gcb.14492, 2019.
- 719 Lobotka, V.: Terraced fields in Slovakia (In Slovak: Terasove polia na Slovensku), Agric., 2(6), 539–549, 1955.
- 720 Long, H. L., Heilig, G. K., Wang, J., Li, X. B., Luo, M., Wu, X. Q. and Zhang, M.: Land use and soil erosion in  
721 the upper reaches of the Yangtze River: Some socio-economic considerations on China’s Grain-for-Green  
722 Programme, L. Degrad. Dev., 17(6), 589–603, doi:10.1002/ldr.736, 2006.
- 723 Loughran, R. J., Elliott, G. L., Campbell, B. L. and Shelly, D. J.: Estimation of soil erosion from caesium-137  
724 measurements in a small, cultivated catchment in Australia, Int. J. Radiat. Appl. Instrumentation. Part, 39(11),  
725 Afshar, F. A., Ayoubi, S., Jalalian, A. (2010)., doi:10.1016/0883-2889(88)90009-3, 1988.
- 726 Luo, Y., Ahlström, A., Allison, S. D., Batjes, N. H., Brovkin, V., Carvalhais, N., Chappell, A., Ciais, P.,  
727 Davidson, E. A., Finzi, A., Georgiou, K., Guenet, B., Hararuk, O., Harden, J. W., He, Y., Hopkins, F., Jiang, L.,  
728 Koven, C., Jackson, R. B., Jones, C. D., Lara, M. J., Liang, J., McGuire, A. D., Parton, W., Peng, C., Randerson,  
729 J. T., Salazar, A., Sierra, C. A., Smith, M. J., Tian, H., Todd-Brown, K. E. O., Torn, M., van Groenigen, K. J.,  
730 Wang, Y. P., West, T. O., Wei, Y., Wieder, W. R., Xia, J., Xu, X., Xu, X. and Zhou, T.: Toward more realistic  
731 projections of soil carbon dynamics by Earth system models, Global Biogeochem. Cycles, 30(1), 40–56,  
732 doi:10.1002/2015GB005239, 2016.
- 733 Mabit, L., Meusburger, K., Fulajtar, E. and Alewell, C.: The usefulness of <sup>137</sup>Cs as a tracer for soil erosion  
734 assessment: A critical reply to Parsons and Foster (2011), Earth-Science Rev., 127, 300–307,  
735 doi:10.1016/j.earscirev.2013.05.008, 2013.
- 736 Mabit, L., Chhem-Kieth, S., Dornhofer, P., Toloza, A., Benmansour, M., Bernard, C., Fulajtar, E. and Walling,  
737 D. E.: <sup>137</sup>Cs: A widely used and validated medium-term soil tracer, in Guidelines for using fallout  
738 radionuclides to assess erosion and effectiveness of soil conservation strategies. IAEA-TECDOC-1741., pp. 27–  
739 78, IAEA, Vienna., 2014.
- 740 McCool, D. K., Foster, G. R., Mutchler, C. K. and Meyer, L. D.: Revised slope length factor for the Universal  
741 Soil Loss Equation, Trans. ASAE, 32, 1571–1576, 1989.
- 742 McDermid, S. S., Mearns, L. O. and Ruane, A. C.: Representing agriculture in Earth System Models:  
743 Approaches and priorities for development, J. Adv. Model. Earth Syst., 9(5), 2230–2265,  
744 doi:10.1002/2016MS000749, 2017.
- 745 Meyer, L. D.: Evolution of the Universal Soil Loss Equation, J. Soil Water Conserv., 39(2), 99–104, 1984.
- 746 Montgomery, D. R.: Soil erosion and agricultural sustainability., Proc. Natl. Acad. Sci. U. S. A., 104(33),  
747 13268–72, doi:10.1073/pnas.0611508104, 2007.
- 748 Morgan, R. P. C.: Soil erosion and conservation, 3rd ed., Blackwell Science Ltd., 2005.
- 749 Mueller, C., Elliott, J., Chryssanthacopoulos, J., Arneth, A., Balkovic, J., Ciais, P., Deryng, D., Folberth, C.,  
750 Glotter, M., Hoek, S., Iizumi, T., Izaurralde, R. C., Jones, C., Khabarov, N., Lawrence, P., Liu, W., Olin, S.,  
751 Pugh, T. A. M., Ray, D. K., Reddy, A., Rosenzweig, C., Ruane, A. C., Sakurai, G., Schmid, E., Skalsky, R.,  
752 Song, C. X., Wang, X., De Wit, A. and Yang, H.: Global gridded crop model evaluation: Benchmarking, skills,  
753 deficiencies and implications, Geosci. Model Dev., 10(4), 1403–1422, doi:10.5194/gmd-10-1403-2017, 2017.
- 754 Mueller, N. D., Gerber, J. S., Johnston, M., Ray, D. K., Ramankutty, N. and Foley, J. A.: Closing yield gaps  
755 through nutrient and water management, Nature, 494(7437), 390–390, doi:10.1038/nature11907, 2012.

- 756 Mutchler, C. K., Murphree, C. E. and McGregor, K. C.: Laboratory and Field Plots for Erosion Research, in Soil  
757 Erosion Research Methods, edited by R. Lal, p. 352, Routledge., 1994.
- 758 Nearing, M. A., Romkens, M. J. M., Norton, L. D., Stott, D. E., Rhoton, F. E., Laflen, J. M., Flanagan, D. C.,  
759 Alonso, C. V., Binger, R. L., Dabney, S. M., Doering, O. C., Huang, C. H., McGregor, K. C. and Simon, A.:  
760 Measurements and models of soil loss rates, *Science* (80-. ), 290(5495), 1300–1301, 2000.
- 761 Nossent, J., Elsen, P. and Bauwens, W.: Sobol’ sensitivity analysis of a complex environmental model, *Environ.*  
762 *Model. Softw.*, 26(12), 1515–1525, doi:10.1016/j.envsoft.2011.08.010, 2011.
- 763 Nyssen, J., Frankl, A., Zenebe, A., Deckers, J. and Poesen, J.: Land Management in the Northern Ethiopian  
764 Highlands: Local and Global Perspectives; Past, Present and Future, *L. Degrad. Dev.*, 26(7), 759–764,  
765 doi:10.1002/ldr.2336, 2015.
- 766 Nyssen, J., Tielens, S., Gebreyohannes, T., Araya, T., Teka, K., van de Wauw, J., Degeyndt, K.,  
767 Descheemaeker, K., Amare, K., Haile, M., Zenebe, A., Munro, N., Walraevens, K., Gebrehiwot, K., Poesen, J.,  
768 Frankl, A., Tsegay, A. and Deckers, J.: Understanding spatial patterns of soils for sustainable agriculture in  
769 northern Ethiopia’s tropical mountains., 2019.
- 770 Onstad, C. A. and Foster, G. R.: Erosion modeling on a watershed, *Trans. ASAE*, 18, 288–292, 1975.
- 771 Van Oost, K., Quine, T. A., Govers, G., Gryze, S. De, Six, J., Harden, J. W., Mccarty, G. W., Heckrath, G.,  
772 Kosmas, C., Giraldez, J. V and Silva, J. R. M.: The Impact of Agricultural Soil Erosion on the Global Carbon  
773 Cycle, *Science* (80-. ), 318(5850), 626–629, 2007.
- 774 Panagos, P., Borrelli, P., Meusburger, K., van der Zanden, E. H., Poesen, J. and Alewell, C.: Modelling the  
775 effect of support practices (P-factor) on the reduction of soil erosion by water at European scale, *Environ. Sci.*  
776 *Policy*, 51, 23–34, doi:10.1016/j.envsci.2015.03.012, 2015.
- 777 Panagos, P., Borrelli, P., Poesen, J., Meusburger, K., Ballabio, C., Lugato, E., Montanarella, L. and Alewell, C.:  
778 Reply to “The new assessment of soil loss by water erosion in Europe. Panagos P. et al., 2015 *Environ. Sci.*  
779 *Policy* 54, 438-447-A response” by Evans and Boardman [*Environ. Sci. Policy* 58, 11-15], *Environ. Sci. Policy*,  
780 59, 53–57, doi:10.1016/j.envsci.2016.02.010, 2016.
- 781 Panagos, P., Standardi, G., Borrelli, P., Lugato, E., Montanarella, L. and Bosello, F.: Cost of agricultural  
782 productivity loss due to soil erosion in the European Union: From direct cost evaluation approaches to the use of  
783 macroeconomic models, *L. Degrad. Dev.*, 29(3), 471–484, doi:10.1002/ldr.2879, 2018.
- 784 Pannell, D. J., Llewellyn, R. S. and Corbeels, M.: The farm-level economics of conservation agriculture for  
785 resource-poor farmers, *Agric. Ecosyst. Environ.*, 187, 52–64, doi:10.1016/j.agee.2013.10.014, 2014.
- 786 Parsons, A.: How reliable are our methods for estimating soil erosion by water?, *Sci. Total Environ.*, 676, 215–  
787 221, 2019.
- 788 Parsons, A. J. and Foster, I. D. L.: The assumptions of science. A reply to Mabit et al. (2013)., *Earth-Science*  
789 *Rev.*, 127, 308–310, doi:10.1016/j.earscirev.2013.05.011, 2013.
- 790 Pelletier, J. D., Broxton, P. D., Hazenberg, P., Zeng, X., Troch, P. A., Niu, G.-Y., Williams, Z., Brunke, M. A.  
791 and Gochis, D.: A gridded global data set of soil, intact regolith, and sedimentary deposit thicknesses for  
792 regional and global land surface modeling, *J. Adv. Model. Earth Syst.*, 8(1), 41–65,  
793 doi:10.1002/2015MS000526, 2016.
- 794 Pimentel, D.: Soil erosion: A food and environmental threat, *Environ. Dev. Sustain.*, 8(1), 119–137,  
795 doi:10.1007/s10668-005-1262-8, 2006.
- 796 Pimentel, D., Harvey, C., Resosudarmo, P., Sinclair, K., Kurz, D., McNair, M., Crist, S., Shpritz, L., Fitton, L.,  
797 Saffouri, R. and Blair, R.: Environmental and economic costs of soil erosion and conservation benefits., *Science*  
798 (80-. ), 267(5201), 1117–1123, doi:10.1126/science.267.5201.1117, 1995.
- 799 De Ploey, J. and Gabriels, D.: Measuring soil loss and experimental studies, in *Soil Erosion*, edited by M. J.  
800 Kirkby and R. P. C. Morgan, pp. 63–108, Wiley, Chichester., 1980.
- 801 Poesen, J., Nachtergaele, J., Verstraeten, G. and Valentin, C.: Gully erosion and environmental change:  
802 Importance and research needs, *Catena*, 50(2–4), 91–133, doi:10.1016/S0341-8162(02)00143-1, 2003.
- 803 Pongratz, J., Dolman, H., Don, A., Erb, K. H., Fuchs, R., Herold, M., Jones, C., Kuemmerle, T., Luysaert, S.,

804 Meyfroidt, P. and Naudts, K.: Models meet data: Challenges and opportunities in implementing land  
805 management in Earth system models, *Glob. Chang. Biol.*, 24(4), 1470–1487, doi:10.1111/gcb.13988, 2018.

806 Portmann, F. T., Siebert, S. and Döll, P.: MIRCA2000—Global monthly irrigated and rainfed crop areas around  
807 the year 2000: A new high-resolution data set for agricultural and hydrological modeling, *Global Biogeochem.*  
808 *Cycles*, 24(1), doi:10.1029/2008GB003435, 2010.

809 Porwollik, V., Rolinski, S., Heinke, J. and Müller, C.: Generating a rule-based global gridded tillage dataset,  
810 *Earth Syst. Sci. Data*, 11(2), 823–843, doi:10.5194/essd-11-823-2019, 2019.

811 Rallison, R. E.: Origin and Evolution of the SCS Runoff Equation, in *Proceeding of the Symposium on*  
812 *Watershed Management '80 American Society of Civil Engineering Boise ID.*, 1980.

813 Renard, K., Foster, G., Weesies, G., McCool, D. and Yoder, D.: Predicting soil erosion by water: a guide to  
814 conservation planning with the Revised Universal Soil Loss Equation (RUSLE), *Agric. Handb. No. 703*, 404,  
815 doi:DC0-16-048938-5 65–100., 1997.

816 Romeo, R., Vita, A., Manuelli, S., Zanini, E., Freppaz, M. and Stanchi, S.: Understanding Mountain Soils: A  
817 contribution from mountain areas to the International Year of Soils 2015, Rome., 2015.

818 Roose, E.: Land husbandry - Components and strategy. 70 FAO soils bulletin, Food and Agriculture  
819 Organization of the United Nations, Rome., 1996.

820 Ruane, A. C., Goldberg, R. and Chryssanthacopoulos, J.: Climate forcing datasets for agricultural modeling:  
821 Merged products for gap-filling and historical climate series estimation, *Agric. For. Meteorol.*, 200, 233–248,  
822 doi:10.1016/j.agrformet.2014.09.016, 2015.

823 Sacks, W. J., Deryng, D., Foley, J. A. and Ramankutty, N.: Crop planting dates: An analysis of global patterns,  
824 *Glob. Ecol. Biogeogr.*, 19(5), 607–620, doi:10.1111/j.1466-8238.2010.00551.x, 2010.

825 Sadeghi, S. H. R. and Mizuyama, T.: Applicability of the Modified Universal Soil Loss Equation for prediction  
826 of sediment yield in Khanmirza watershed, Iran, *Hydrol. Sci. J.*, 52(5), 1068–1075, doi:10.1623/hysj.52.5.1068,  
827 2007.

828 Scherer, L. and Pfister, S.: Modelling spatially explicit impacts from phosphorus emissions in agriculture, *Int. J.*  
829 *Life Cycle Assess.*, 20(6), 785–795, doi:10.1007/s11367-015-0880-0, 2015.

830 Sharpley, A. N. and Williams, J. R.: EPIC — Erosion / Productivity Impact Calculator: 1. Model  
831 Documentation, U.S. Dep. Agric. Tech. Bull., 1768, 235, 1990.

832 Skalský, R., Tarasovičová, Z., Balkovič, J., Schmid, E., Fuchs, M., Moltchanova, E., Kindermann, G. and  
833 Scholtz, P.: GEO-BENE global database for bio-physical modeling. GEOBENE project. [online] Available  
834 from: [http://geo-bene.project-archive.iiasa.ac.at/files/Deliverables/Geo-BeneGlbDb10\(DataDescription\).pdf](http://geo-bene.project-archive.iiasa.ac.at/files/Deliverables/Geo-BeneGlbDb10(DataDescription).pdf),  
835 2008.

836 Sobol, I. M.: On sensitivity estimation for nonlinear mathematical models, *Matem. Mod.*, 2, 112–118, 1990.

837 Stroosnijder, L.: Measurement of erosion: Is it possible?, *Catena*, 64(2–3), 162–173,  
838 doi:10.1016/j.catena.2005.08.004, 2005.

839 Terranova, O., Antronico, L., Coscarelli, R. and Iaquinta, P.: Soil erosion risk scenarios in the Mediterranean  
840 environment using RUSLE and GIS: An application model for Calabria (southern Italy), *Geomorphology*,  
841 112(3–4), 228–245, doi:10.1016/j.geomorph.2009.06.009, 2009.

842 Trimble, S. W. and Crosson, P.: U.S. Soil Erosion Rates--Myth and Reality, *Science (80-. )*, 289(5477), 248–  
843 250, doi:10.1126/science.289.5477.248, 2000.

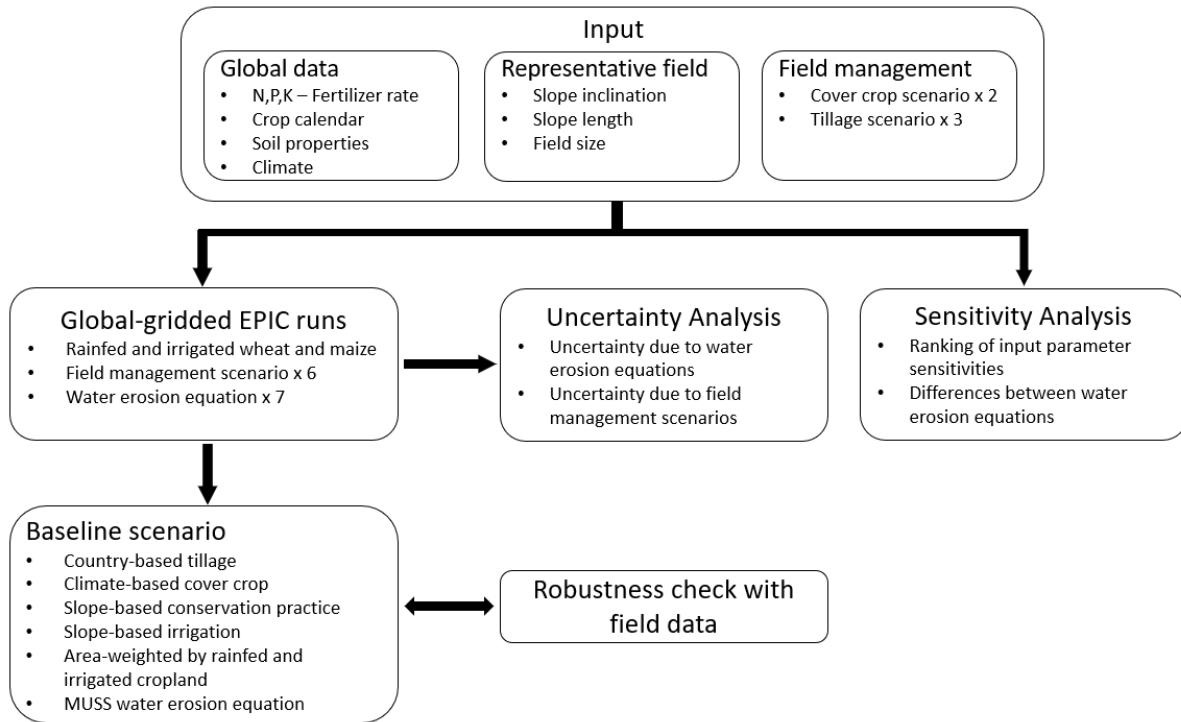
844 Turkelboom, F., Poesen, J. and Trébuil, G.: The multiple land degradation effects caused by land-use  
845 intensification in tropical steepplands: A catchment study from northern Thailand, *Catena*, 75(1), 102–116,  
846 doi:10.1016/j.catena.2008.04.012, 2008.

847 UN: Standard Country or Area Codes for Statistical Use (Revision 4). Series M, No. 49/Rev.4, New York.,  
848 1999.

849 USDA-ARC: Science documentation. Revised Universal Soil Loss Equation, Version 2 (RUSLE 2),  
850 Washington, D.C., 2013.

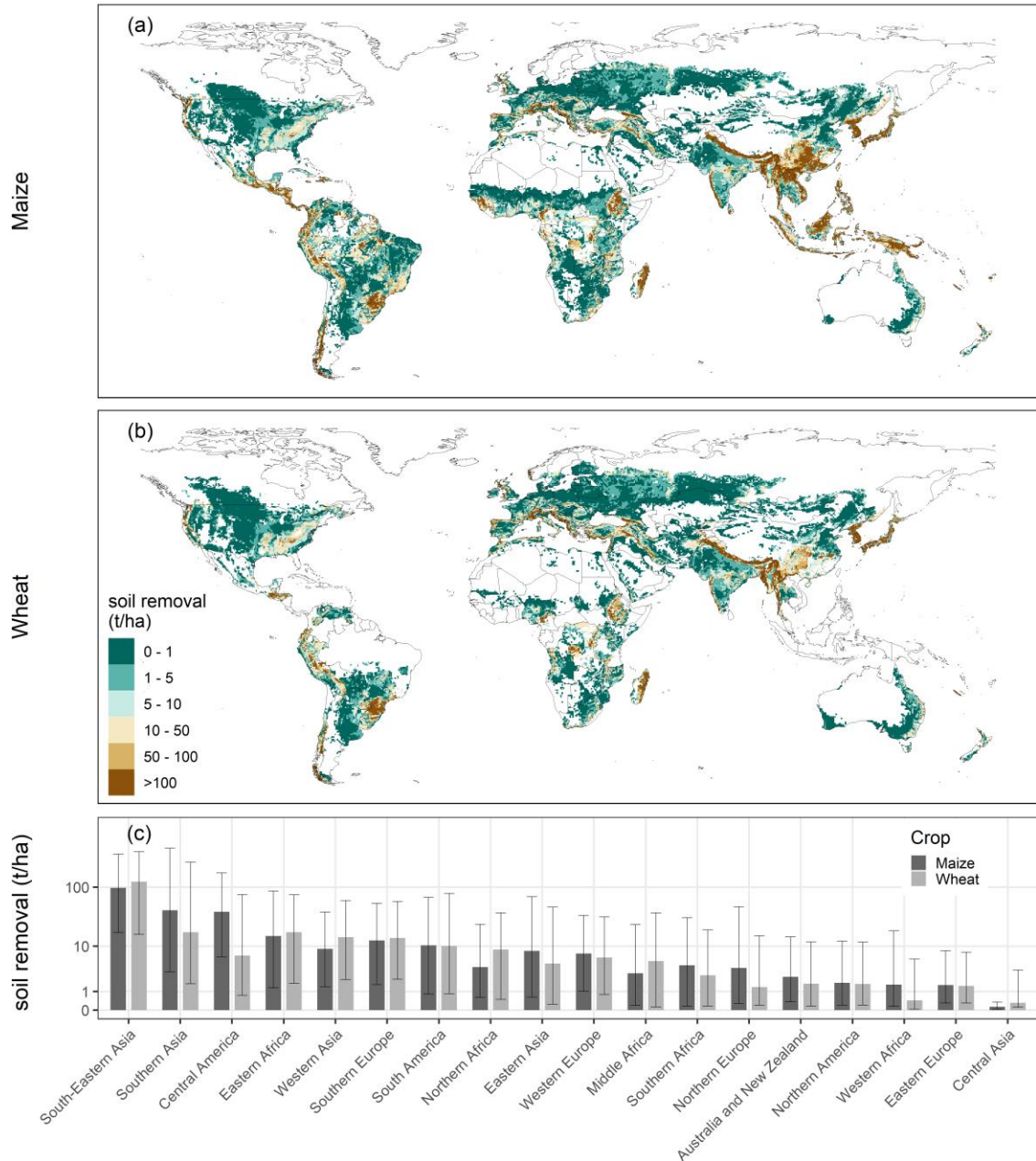


- 851 USGS: USGS 30 ARC-second Global Elevation Data, GTOPO30, 1997.
- 852 Vâje, P. I., Singh, B. R. and Lal, R.: Soil Erosion and Nutrient Losses from a Volcanic Ash Soil in Kilimanjaro  
853 Region, Tanzania, *J. Sustain. Agr.*, 26(4), 23–42, doi:10.1300/J064v26n04, 2005.
- 854 Valentin, C., Agus, F., Alamban, R., Boosaner, A., Bricquet, J. P., Chaplot, V., de Guzman, T., de Rouw, A.,  
855 Janeau, J. L., Orange, D., Phachomphonh, K., Do Duy Phai, Podwojewski, P., Ribolzi, O., Silvera, N.,  
856 Subagyono, K., Thiébaux, J. P., Tran Duc Toan and Vadari, T.: Runoff and sediment losses from 27 upland  
857 catchments in Southeast Asia: Impact of rapid land use changes and conservation practices, *Agric. Ecosyst.*  
858 *Environ.*, 128(4), 225–238, doi:10.1016/j.agee.2008.06.004, 2008.
- 859 Walling, D. E. and Webb, B. W.: Erosion and sediment yield: a global overview, *IAHS Publ. Proc. Reports-*  
860 *Intern Assoc Hydrol. Sci.*, 236(236), 3–20 [online] Available from:  
861 [http://books.google.com/books?hl=en&lr=&id=bZ-](http://books.google.com/books?hl=en&lr=&id=bZ-ufVQV5yAC&oi=fnd&pg=PA3&dq=Erosion+and+sediment+yield:+a+global+overview&ots=u-QfIZyy5V&sig=iFyBdzc5dvvd-rF0T35j1jn5EZg)  
862 [ufVQV5yAC&oi=fnd&pg=PA3&dq=Erosion+and+sediment+yield:+a+global+overview&ots=u-](http://books.google.com/books?hl=en&lr=&id=bZ-ufVQV5yAC&oi=fnd&pg=PA3&dq=Erosion+and+sediment+yield:+a+global+overview&ots=u-QfIZyy5V&sig=iFyBdzc5dvvd-rF0T35j1jn5EZg)  
863 [QfIZyy5V&sig=iFyBdzc5dvvd-rF0T35j1jn5EZg](http://books.google.com/books?hl=en&lr=&id=bZ-ufVQV5yAC&oi=fnd&pg=PA3&dq=Erosion+and+sediment+yield:+a+global+overview&ots=u-QfIZyy5V&sig=iFyBdzc5dvvd-rF0T35j1jn5EZg), 1996.
- 864 Walling, D. E., He, Q. and Zhang, Y.: Conversion Models And Related Software, in *Guidelines for Using*  
865 *Fallout Radionuclides to Assess Erosion and Effectiveness of Soil Conservation Strategies*, IAEA, Vienna.,  
866 2014.
- 867 Wang, X., Kemanian, A. R., Williams, J. R., Ahuja, L. R. and Ma, L.: Special Features of the EPIC and APEX  
868 Modeling Package and Procedures for Parameterization, Calibration, Validation, and Applications, , 16802,  
869 doi:10.2134/advagricsystmodel2.c6, 2011.
- 870 Watson, A. and Evans, R.: A comparison of estimates of soil erosion made in the field and from photographs,  
871 *Soil Tillage Res.*, 19, 17–27, 1991.
- 872 Williams, J. R.: Sediment yield prediction with universal equation on using runoff energy factor., in *Present and*  
873 *prospective technology for predicting sediment yields and sources*, ARS S-40, pp. 244–252, USDA-ARS,  
874 Washington.D.C., 1975.
- 875 Williams, J. R.: The Erosion-Productivity Impact Calculator (EPIC) Model: A Case History, *Philos. Trans. R.*  
876 *Soc. B Biol. Sci.*, 329(1255), 421–428, doi:10.1098/rstb.1990.0184, 1990.
- 877 Williams, J. R.: The EPIC model, in *Computer Models of Watershed Hydrology*, edited by V. P. Singh, pp.  
878 909–1000, Water Resources Publications., 1995.
- 879 Williams, J. R., Izaurralde, R. C. and Steglich, E. M.: *Agricultural Policy/Environmental eXtender Model*,  
880 *Theoretical documentation version 0806.*, 2012.
- 881 Wischmeier, W. H. and Smith, D. D.: Predicting rainfall erosion losses, *Agric. Handb. no. 537*, (537), 285–291,  
882 doi:10.1029/TR039i002p00285, 1978.
- 883 Zachar, D.: *Soil Erosion*, Elsevier, Amsterdam., 1982.
- 884 Zapata, F.: *Handbook for the Assessment of Soil Erosion and Sedimentation Using Environmental*  
885 *Radionuclides*, Dordrecht., 2002.
- 886
- 887



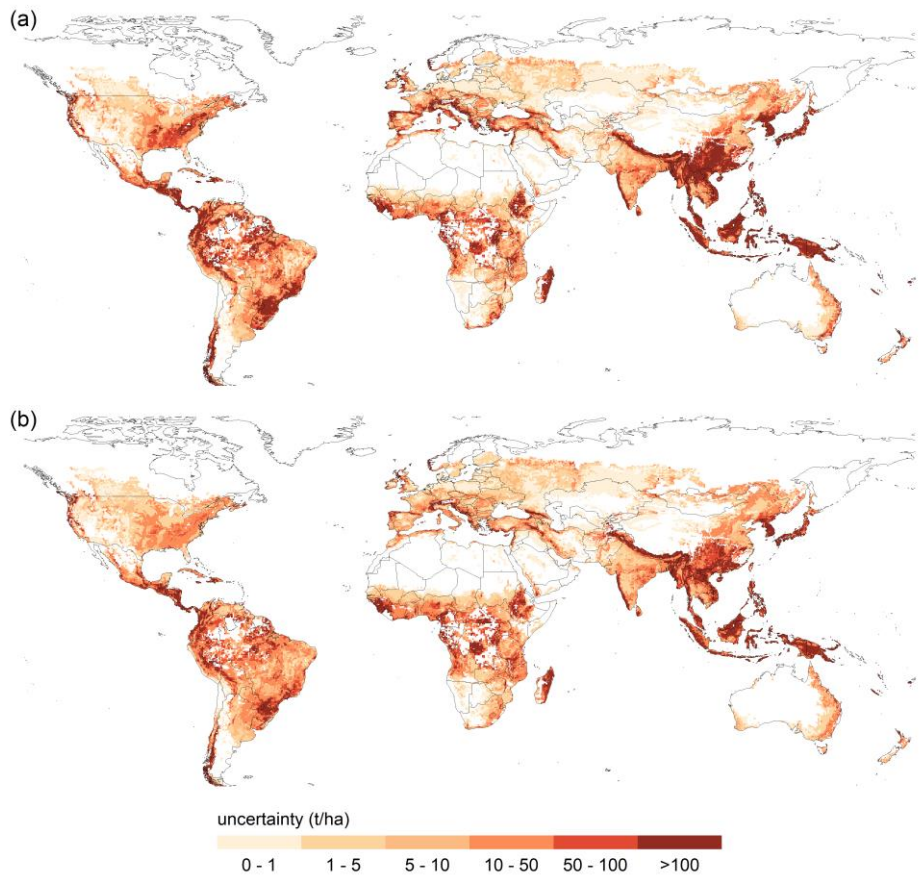
888

889 Figure 1: Scheme of procedure used for simulating global water erosion with EPIC-IIASA and for analysing the  
 890 uncertainty, sensitivity and robustness of our simulation setup.



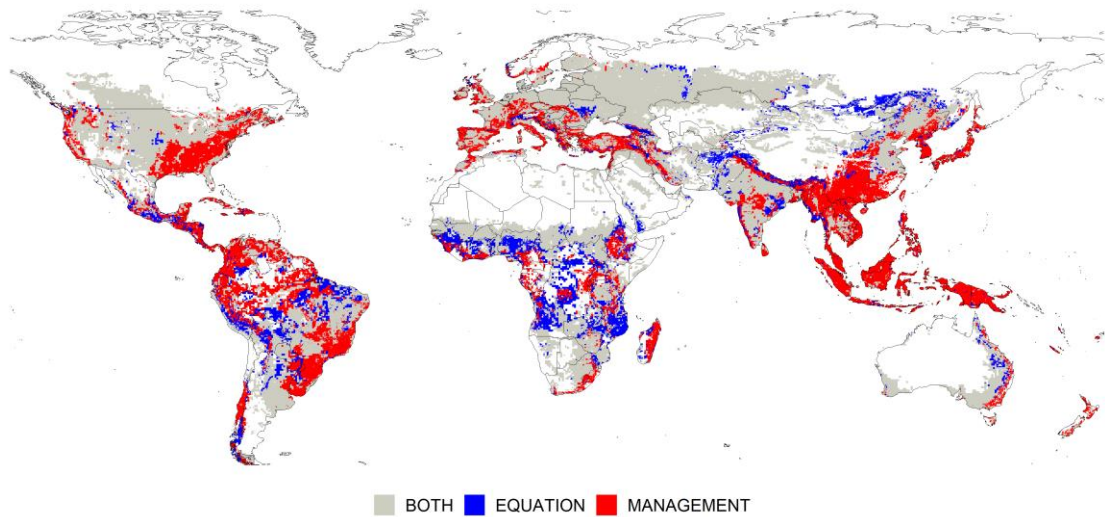
891

892 Figure 2: Soil loss due to water erosion in maize (a) and wheat (b) fields simulated with the baseline scenario.  
 893 Each pixel cell illustrates the median relative water erosion of one representative field. The extent of cropland  
 894 areas is not considered in pixel cell size. The bars in the bottom plot (c) illustrate median soil removal for major  
 895 world regions simulated under maize and wheat cultivation. The lines and whiskers illustrate 25th and 75th  
 896 percentile values. The classification of world regions is illustrated in Fig. S3. Due to the large gap between  
 897 aggregated values, all values in the bottom plot have been log-transformed to facilitate the visual comparison.



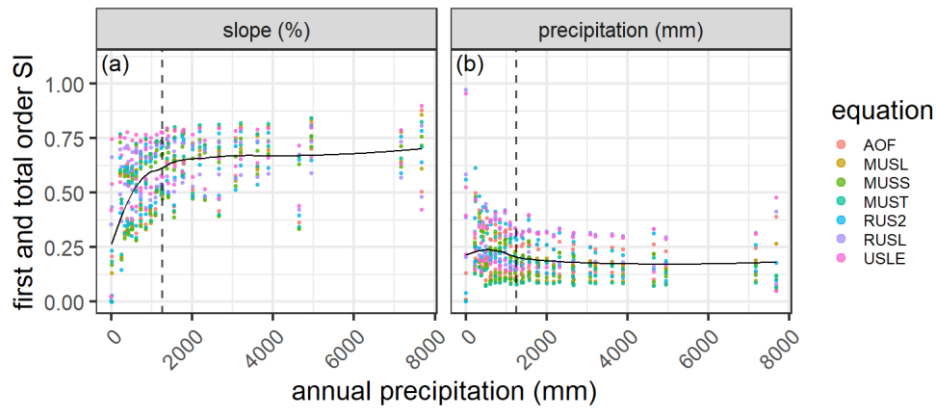
898

899 Figure 3: Water erosion uncertainty due to (a) field management assumptions and (b) water erosion equations.



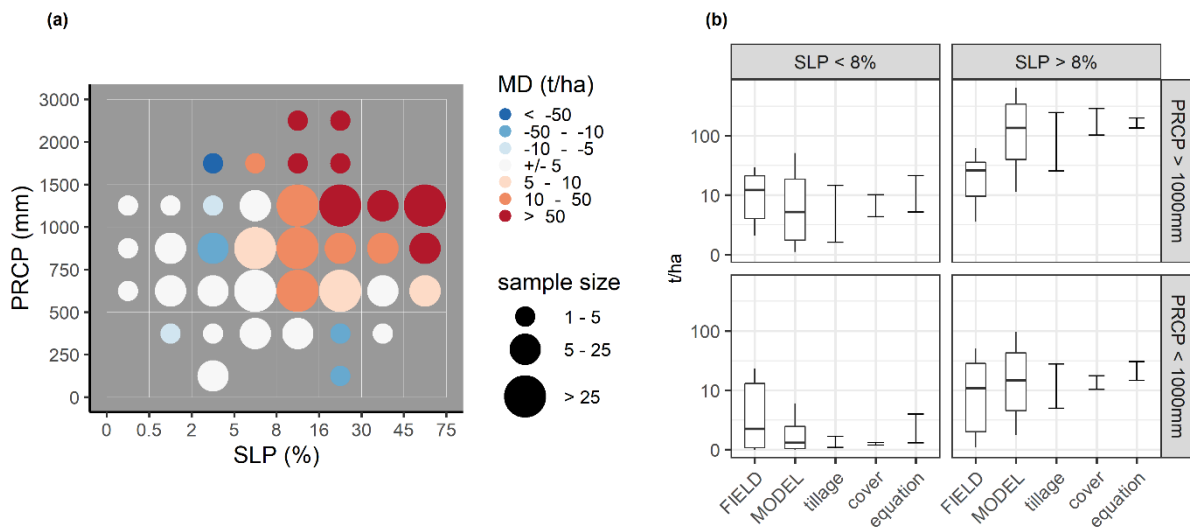
900

901 Figure 4: Prevailing uncertainty, defined as the higher uncertainty range by at least 5 t ha<sup>-1</sup>.



902

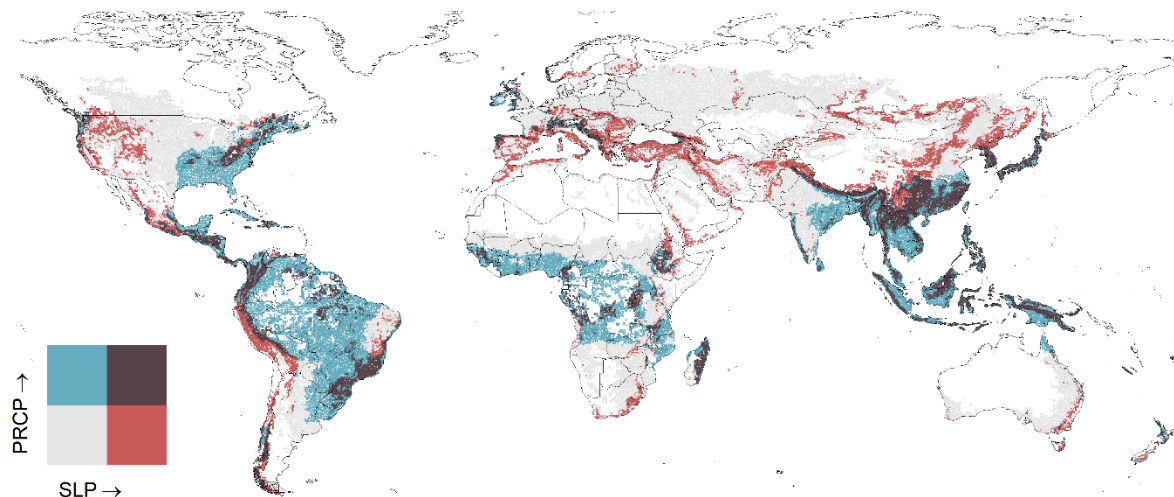
903 Figure 5: First-order and total-order sensitivity indices (SI) for (a) slope steepness (%) and (b) precipitation  
 904 [mm]. The dashed vertical line illustrates median annual precipitation at all tested locations (1248 mm).



905

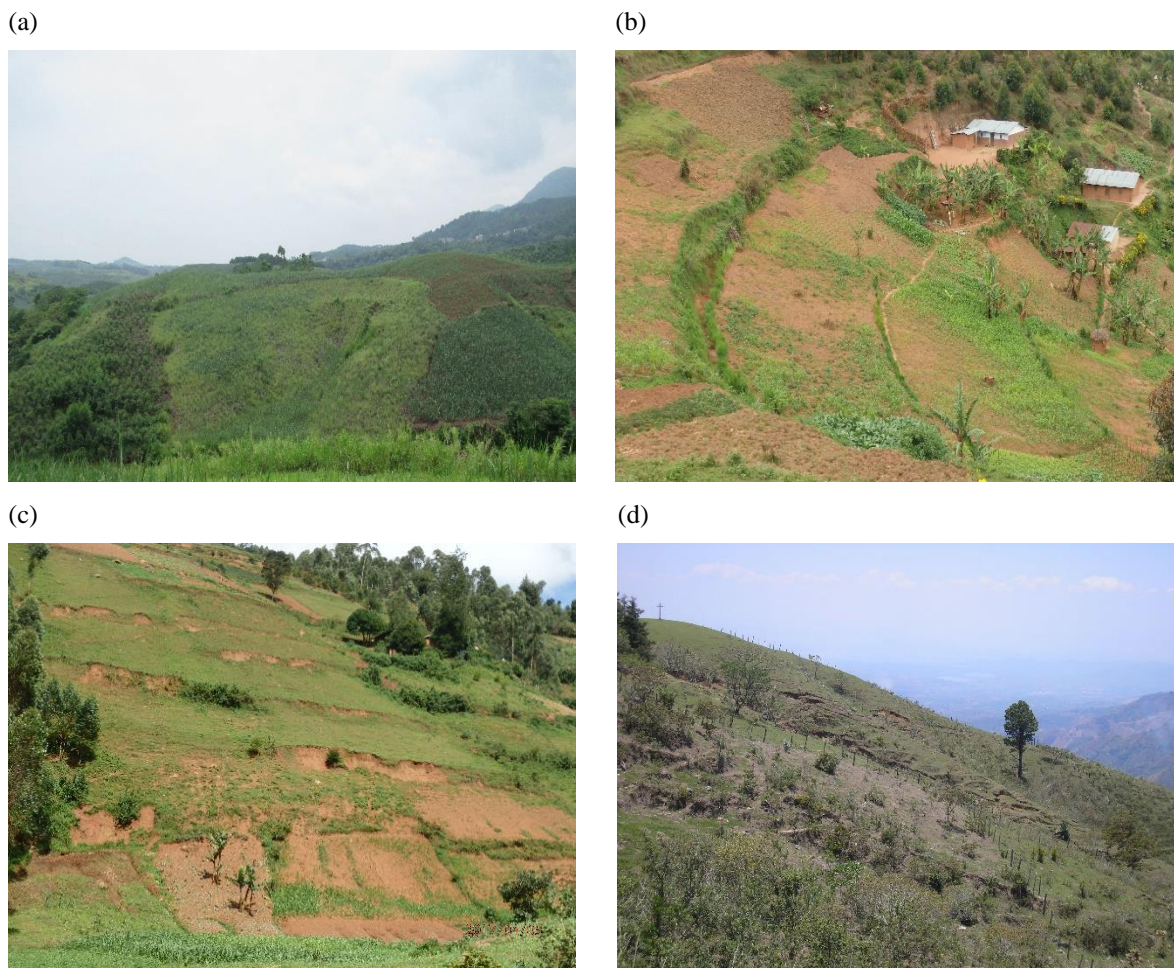
906 Figure 6: Comparison of simulated erosion with measured erosion. (a) Median deviation (MD) in  $t\ ha^{-1}$  between  
 907 simulated erosion using the baseline scenario and measured erosion. Simulated and measured data is grouped  
 908 into precipitation classes and slope classes used for the simulation setup. (b) Distributions of measured erosion  
 909 rates, erosion rates simulated with the baseline scenario and uncertainty ranges for management assumptions  
 910 and erosion equations. The boxplots are defined by the median, the 25<sup>th</sup> and the 75<sup>th</sup> percentile of simulated and  
 911 measured erosion rates. Whiskers illustrate the 10<sup>th</sup> and 90<sup>th</sup> percentile. The three bars next to the boxplots  
 912 illustrate minimum and maximum median erosion rates calculated with all tillage and cover crop scenarios and  
 913 with all water erosion equations. The values have been log-transformed for better visualization.





914

915 Figure 7: Distribution of low to high slope steepness (SLP) and annual precipitation (PRCP) in maize and wheat  
 916 fields. Dark areas illustrate grid cells where dominant slopes are steeper than 8 % and annual precipitation is above  
 917 1000 mm. Correspondingly, blue, red, and grey pixels are below one or both thresholds.



918 Figure 8: (a) Sugar cane cultivation on steep slopes in South China ([Nanning, Guangxi Zhuang Autonomous](#)  
 919 [Region](#)). ~~(The steepest slopes are already abandoned and reforested by eucalyptus trees).~~ (b) Maize cultivation  
 920 on strongly eroded slopes (30 – 60 %)- in South West Uganda ([Kigwa, Kabale District](#)). (c) Abandoned fields  
 921 and maize cultivation on a steep slope (30 – 60 %) in South West Uganda ([Kigwa, Kabale District](#)). (d)

922 Degraded and abandoned maize fields on steep slopes (20 – 60 %) in Northern El Salvador ([San Ignacio,](#)  
 923 [Chalatenango Department](#)). [The photos and additional examples are provided in Fig. S10 – S17.](#)

924

925 Table 1: Equations for calculating the erosivity factor in each water erosion equation available in EPIC.

Erosivity factor	Equation
$R = EI$ (2)	USLE, RUSLE, RUSLE2 (Renard et al., 1997; USDA-ARC, 2013; Wischmeier and Smith, 1978)
$R = 0.646 * EI + 0.45 * (Q * q_p)^{0.33}$ (3)	AOF (Onstad and Foster, 1975)
$R = 1.586 * (Q * q_p)^{0.56} * WSA^{0.12}$ (4)	MUSLE (Williams 1975)
$R = 2.5 * Q * q_p^{0.5}$ (5)	MUST (Williams, 1995)
$R = 0.79 * (Q * q_p)^{0.65} * WSA^{0.009}$ (6)	MUSS (Williams, 1995)

926

927 Table 2: Tillage management scenarios for maize and wheat cultivation

	Conventional tillage	Reduced tillage	No-tillage
total cultivation operations	6 – 7	4 – 5	3
max. surface roughness	30 – 50 mm	20 mm	10 mm
max. tillage depth	150 mm	150 mm	40 – 60 mm
plant residues left	25 %	50 %	75 %
cover treatment class	straight	contoured	contoured & terraced

928

929 Table 3: Management assumptions and erosion equation selected for the baseline scenario

Option	Baseline			
TILLAGE	<ul style="list-style-type: none"> <li>Mix of conventional, reduced and no-tillage in regions where the national share of conservation agriculture is &gt; 5 % according to the latest reported data in AQUASTAT (2007-2014) (FAO, 2016): Argentina, Australia, Bolivia, Brazil, Canada, Chile, China, Colombia, Finland, Italy, Kazakhstan, New Zealand, Paraguay, Spain, USA, Uruguay, Venezuela, Zambia and Zimbabwe.</li> <li>Mix of conventional and reduced tillage in the rest of the world.</li> </ul>			
OFF-SEASON COVER	<ul style="list-style-type: none"> <li>Cultivation only with cover crops in tropics according to Koeppen-Geiger regions (Fig. S1) (Kottek et al., 2006).</li> <li>Mix of off-season cover with and without cover crops in temperate and cold zones.</li> <li>No cover crops in arid regions.</li> </ul>			
CONSERVATION PRACTICE FACTOR	Slope	0 – 16 %	16 – 30 %	> 30 %
	P-Factor	1.0	0.5	0.15
CROP	Water erosion is simulated in wheat and maize fields based on the global crop distribution by MIRCA2000 (Fig. S2) (Portmann et al., 2010).			

IRRIGATION	<ul style="list-style-type: none"> <li>• Only on slopes <math>\leq 5\%</math>.</li> <li>• Weighted average of irrigated and rainfed cropland based on MIRCA2000 (Portmann et al., 2010).</li> </ul>
METHOD	MUSS water erosion equation.
AGGREGATION	Median of all management scenarios per grid cell and region

930

931 Table 4: First-order sensitivity indices (SI) ranking for the five most sensitive input parameters (PARM) for each  
932 water erosion equation including slope steepness (SLP), daily precipitation (PRCP), soil hydrologic group (HSG),  
933 land use number (LUN), soil silt content (SILT), soil sand content (SAND), curve number parameter (S301),  
934 maximum air temperature (TMX) and crop residues left after harvest (ORHI). The sensitivity indices of the  
935 remaining parameters are presented in Table S3.

rank	AOF		MUSL		MUSS		MUST		RUSLE2		RUSLE		USLE	
	PARM	SI	PARM	SI	PARM	SI	PARM	SI	PARM	SI	PARM	SI	PARM	SI
1	SLP	0.47	SLP	0.47	SLP	0.46	SLP	0.48	SLP	0.46	SLP	0.50	SLP	0.54
2	PRCP	0.13	PRCP	0.10	PRCP	0.12	PRCP	0.09	PRCP	0.16	PRCP	0.20	PRCP	0.18
3	HSG	0.03	HSG	0.04	HSG	0.05	HSG	0.04	HSG	0.03	SAND	0.05	SILT	0.02
4	SILT	0.02	LUN	0.02	LUN	0.02	LUN	0.02	SAND	0.01	TMX	0.01	TMX	0.01
5	LUN	0.01	SILT	0.02	S301	0.01	SILT	0.02	LUN	0.01	ORHI	0.01	ORHI	0.01
...	...	...	...	...	...	...	...	...	...	...	...	...	...	...
<b>sum</b>		0.69		0.68		0.71		0.69		0.71		0.78		0.77

936

937

938 Table 5: Total-order sensitivity indices (SI) ranking for the five most sensitive input parameters (PARM) for each  
939 water erosion equation including slope steepness (SLP), daily precipitation (PRCP), soil hydrologic group (HSG),  
940 land use number (LUN), soil silt content (SILT), soil sand content (SAND), maximum air temperature (TMX)  
941 and crop residues left after harvest (ORHI). The sensitivity indices of the remaining parameters are presented in  
942 Table S3.

rank	AOF		MUSL		MUSS		MUST		RUSLE2		RUSLE		USLE	
	PARM	SI	PARM	SI	PARM	SI	PARM	SI	PARM	SI	PARM	SI	PARM	SI
1	SLP	0.68	SLP	0.68	SLP	0.63	SLP	0.68	SLP	0.66	SLP	0.69	SLP	0.75
2	PRCP	0.28	PRCP	0.23	PRCP	0.22	PRCP	0.21	PRCP	0.32	PRCP	0.36	PRCP	0.36
3	HSG	0.09	HSG	0.12	HSG	0.13	HSG	0.12	HSG	0.08	SAND	0.12	SILT	0.05
4	SILT	0.07	LUN	0.07	LUN	0.07	LUN	0.07	LUN	0.05	TMX	0.02	TMX	0.02
5	LUN	0.05	SILT	0.07	SILT	0.05	SILT	0.07	SAND	0.04	ORHI	0.01	SAND	0.01
...	...	...	...	...	...	...	...	...	...	...	...	...	...	...
<b>sum</b>		1.29		1.30		1.25		1.27		1.34		1.27		1.27

943



1 Text S1.

2 The following equations describe the calculation of the cover and management factor, the soil erodibility factor  
3 and the topographic factor of each water erosion equation:

4 The **cover and management factor** is calculated the same way for each equation:

$$5 \quad C = FRSD * FBIO * FRUF \quad (1)$$

6 where FRSD is the crop residue factor, FBIO is the growing biomass factor and FRUF is the soil random  
7 roughness factor, which are calculated with the following equations (Wang et al., 2011; Williams et al., 2012):

$$8 \quad FRSD = \exp(-P23 * CVRS) \quad (2)$$

$$9 \quad FBIO = 1 - \frac{STL}{(STL + \exp(SCR P1(23) - SCR P2(23) * STL))} * \exp(-P26 * CPHT) \quad (3)$$

$$10 \quad FRUF = \exp(-0.026 * (RR - 6.1)) \quad (4)$$

11 where P23 is an exponential coefficient ranging from 0.01-0.5, CVRS is the amount of above ground crop  
12 residue [t ha<sup>-1</sup>], STL is the amount of standing live biomass of the crop [t ha<sup>-1</sup>], SCR P1(23) and SCR P2(23) are  
13 coefficients defining an S-shaped growth curve used to estimate the fraction of the ground covered by the plant  
14 as a function of the Leaf Area Index, P26 is an exponential coefficient ranging from 0.01-0.2, CPHT is the crop  
15 height [m] and RR is the soil surface random roughness [mm].

16 The **soil erodibility factor** is calculated the same way for the USLE, AOF, MUSLE, MUST and MUSS  
17 equation using a function of sand, silt, clay and organic carbon contents in the soil:

$$18 \quad K = X1 * X2 * X3 * X4 \quad (5)$$

$$19 \quad X1 = 0.2 + 0.3 * \exp(-0.0256 * SAND * (1 - 0.01 * SILT)) \quad (6)$$

$$20 \quad X2 = \left( \frac{SILT}{CLAY + SILT} \right)^{0.3} \quad (7)$$

$$21 \quad X3 = \frac{1 - 0.25 * OC}{OC + \exp(3.718 - 2.947 * OC)}, \text{ IF } OC \leq 5 \quad (8)$$

$$22 \quad X3 = 0.75, \text{ IF } OC > 5 \quad (9)$$

$$23 \quad X4 = \frac{1 - 0.7 * SN1}{SN1 + \exp(-5.509 + 22.899 * SN1)} \quad (10)$$

$$24 \quad SN1 = 1 - 0.01 * SAND \quad (11)$$

25 Where SAND, SILT, CLAY, and OC are the sand, silt, clay, and organic carbon contents of the soil in %. For  
26 the RUSLE and RUSLE2 method soil erodibility is calculated without the organic carbon contents of the soil  
27 using the following equation:

$$28 \quad KR = 9.811 * \left( 0.0034 + 0.0405 * \exp \left( -0.5 * \left( \frac{\log_{10}(DG) + 1.659}{0.7101} \right)^2 \right) \right) \quad (12)$$

29  $DG = exp (SUM) \quad (13)$

30  $SUM = \frac{SAND*0.0247-SILT*3.65-CLAY*6.908}{100} \quad (14)$

31 The **topographic factor** is calculated the same way for the USLE, AOF, MUSLE, MUST and MUSS equation  
 32 using a function of slope length and slope steepness:

33  $LS = \left(\frac{SLPL}{22.127}\right)^{XM} * (SLP * (65.41 * SLP + 4.56) + 0.065) \quad (15)$

34  $XM = 0.3 * \frac{SLP}{SLP + \exp(-1.47 - 61.09 * SLP)} + 0.2 \quad (16)$

35 Where SLPL is the slope length in m, SLP is the land surface slope in m/m and XM is an exponent dependent  
 36 upon slope. The topographic factor for the RUSLE method is calculated using a function of slope length and  
 37 slope steepness as well:

38  $LSR = RSF * RLF \quad (17)$

39  $RSF = 10.8 * SLP + 0.03, \text{ IF } SLPL > 4.57 \ \& \ SLP < 0.09 \quad (18)$

40  $RSF = 16.8 * SLP - 0.5, \text{ IF } SLPL > 4.57 \ \& \ SLP > 0.09 \quad (19)$

41  $RSF = X1, \text{ IF } SLPL < 4.57 \quad (20)$

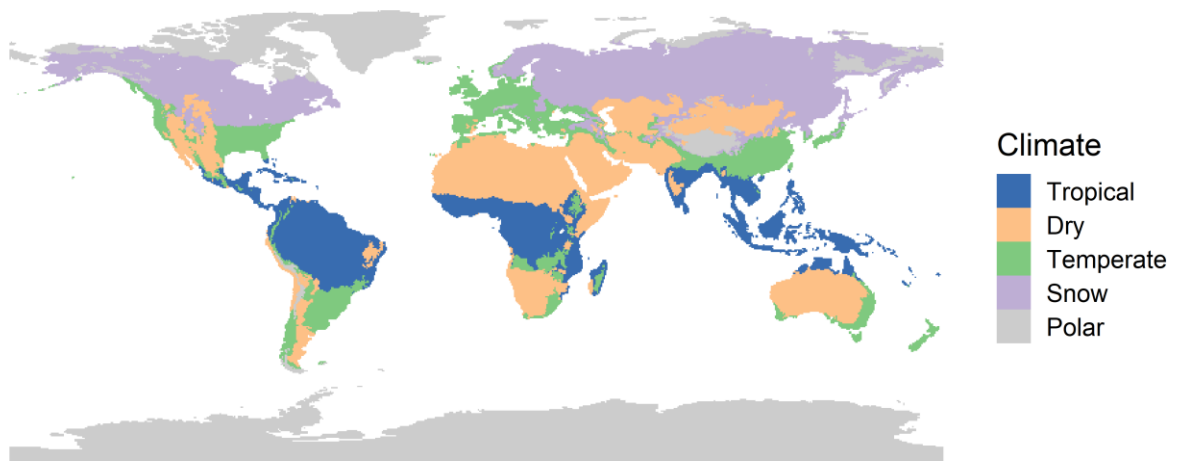
42  $X1 = 3 * SLP^{0.8} + 0.56 \quad (21)$

43  $RLF = \frac{SLPL^{RXM}}{22.127} \quad (22)$

44  $RXM = \frac{B}{1+B} \quad (23)$

45  $B = \frac{SLP}{0.0896 * X1} \quad (24)$

46 Where SLPL is slope length in m and SLP is land surface slope in m/m. The slope steepness factor RSF is  
 47 adjusted for different slope steepness and slope length thresholds based on experimental data (Renard et al.,  
 48 1997). The slope length factor RLF includes an exponent RXM, which is a function of the ratio B of rill erosion  
 49 caused by flow and interrill erosion caused by raindrop impact (USDA-ARC, 2013). B reflects how steepness  
 50 affects rill erosion differently than it does interrill erosion. Rill erosion is assumed to vary linearly with  
 51 steepness. The topographic factor for the RUSLE2 method is calculated the same way than for the RUSLE  
 52 equation if the transport capacity determined by a function of flow rate and slope steepness exceeds sediment  
 53 load. When sediment load exceeds transport capacity RUSLE2 computes deposition. Interrill erosion is assumed  
 54 to occur even when RUSLE2 computes deposition, which can be calculated without a distance term as  
 55 detachment is solely caused by impacting raindrops (USDA-ARC, 2013). Therefore, the slope length factor is  
 56 not considered in the RUSLE2 equation when deposition occurs.

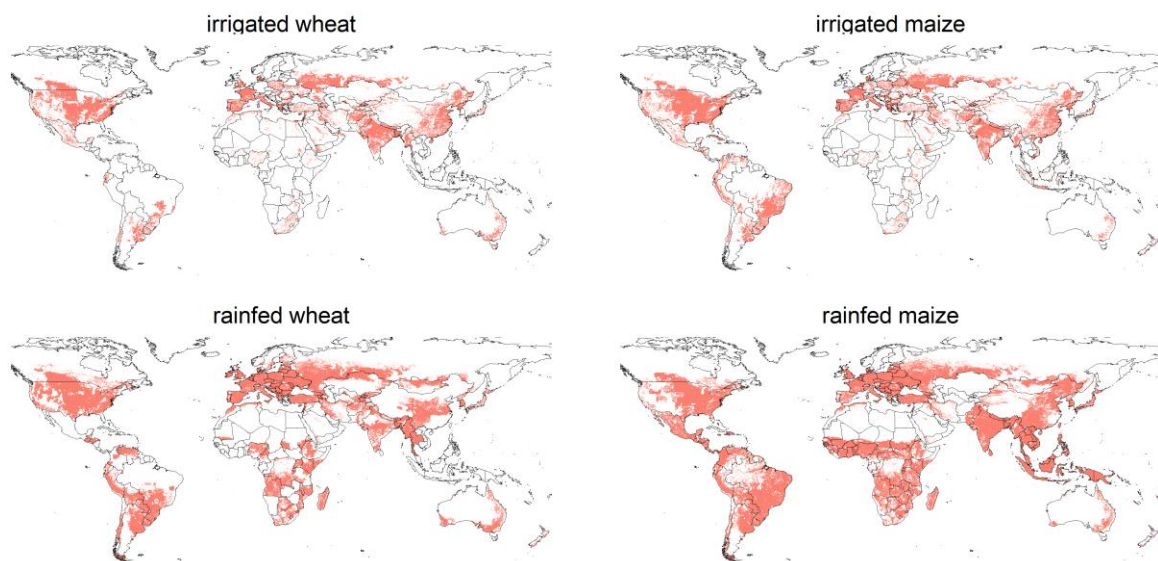


57

58 Figure S1: Main climate zones using the updated Koeppen-Geiger climate classification (Peel et al., 2007).

59

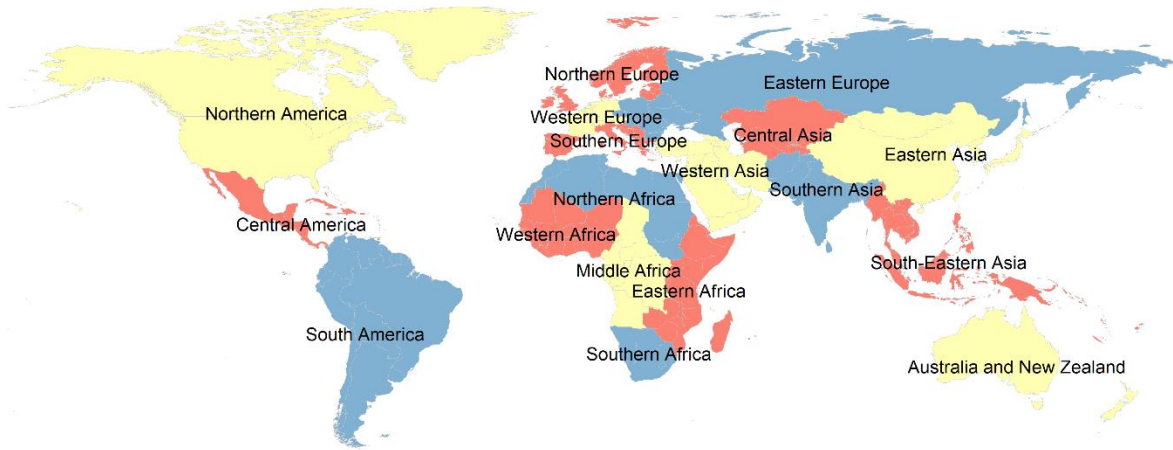
60



61

62 Figure S2: Grid cells with irrigated and rainfed wheat and maize cultivation around the year 2000 (Portmann et  
63 al., 2010).

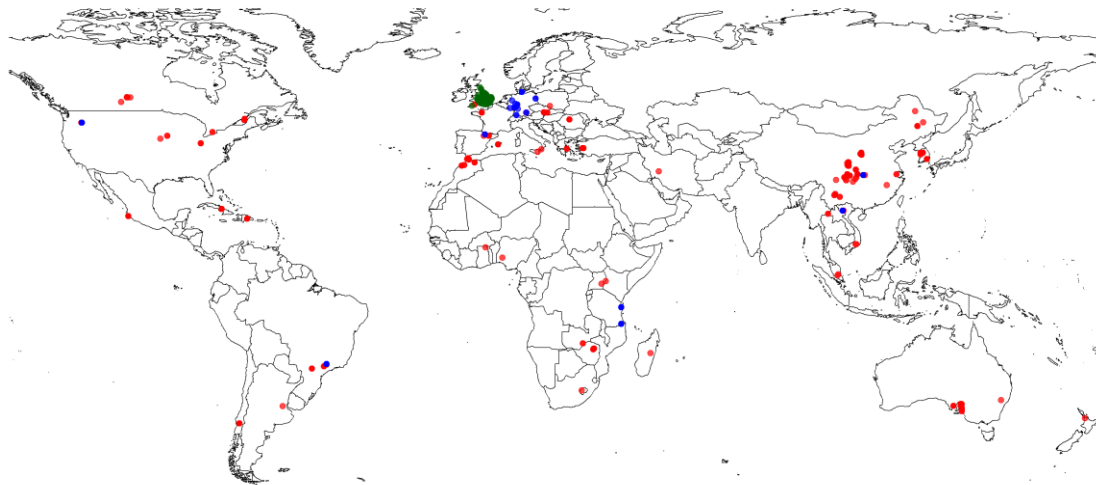
64



65

66 Figure S3: World regions classified using the United Nations geoscheme (UN, 1999) with minor modifications:  
 67 Melanesia has been added to Southeastern Asia and the Caribbean has been added to Central America.

68



method

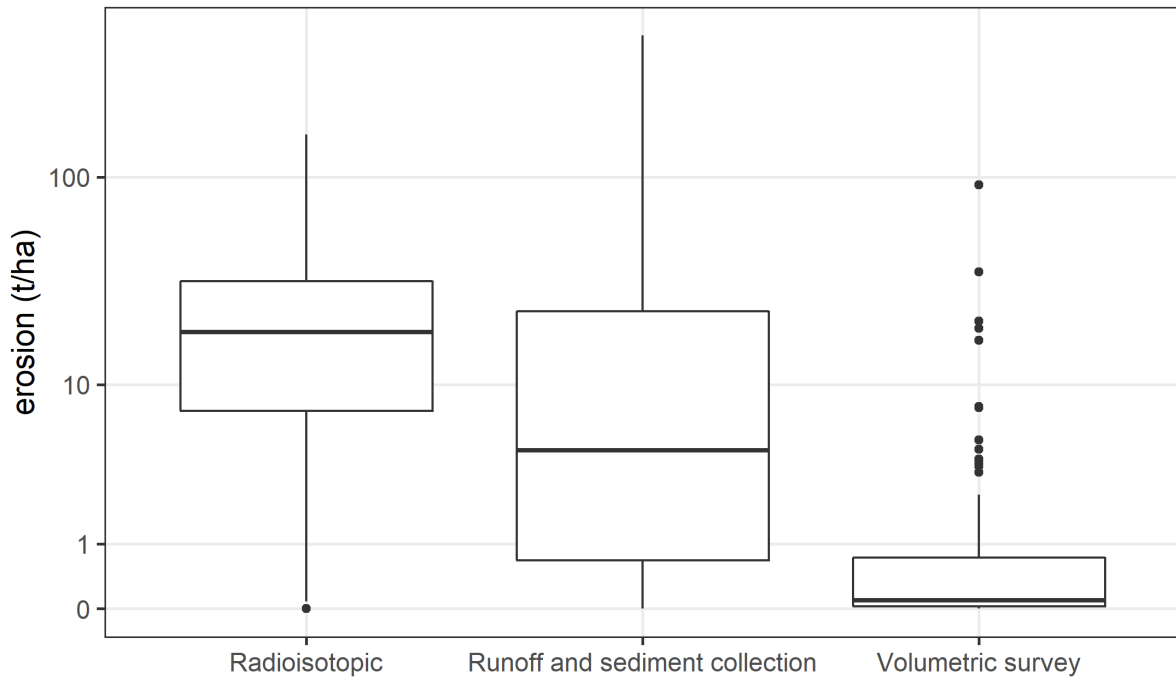
● Radioisotopic ● Runoff and sediment collection ● Volumetric survey

69

70 Figure S4: Locations of water erosion field data from cropland where coordinates were recorded (n=554).

71

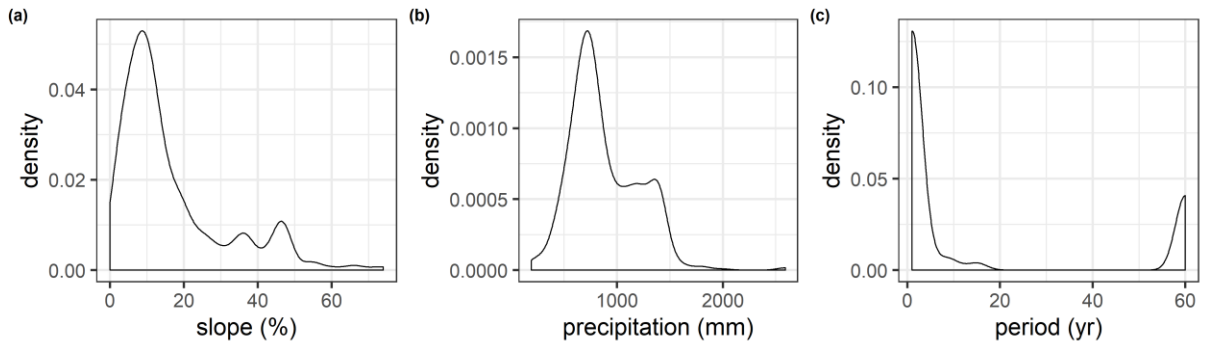
72



73

74 Figure S5: Distribution of erosion values ( $t\ ha^{-1}$ ) measured in agricultural fields using  $^{137}Cs$  method ( $n = 315$ ,  
 75 Mean =  $24\ t\ ha^{-1}$ ; Median =  $18\ t\ ha^{-1}$ ), runoff and sediment collection ( $n = 188$ , Mean =  $21\ t\ ha^{-1}$ ; Median =  $4\ t$   
 76  $ha^{-1}$ ) and volumetric surveys ( $n = 103$ , Mean =  $2\ t\ ha^{-1}$ ; Median =  $0.1\ t\ ha^{-1}$ ).

77

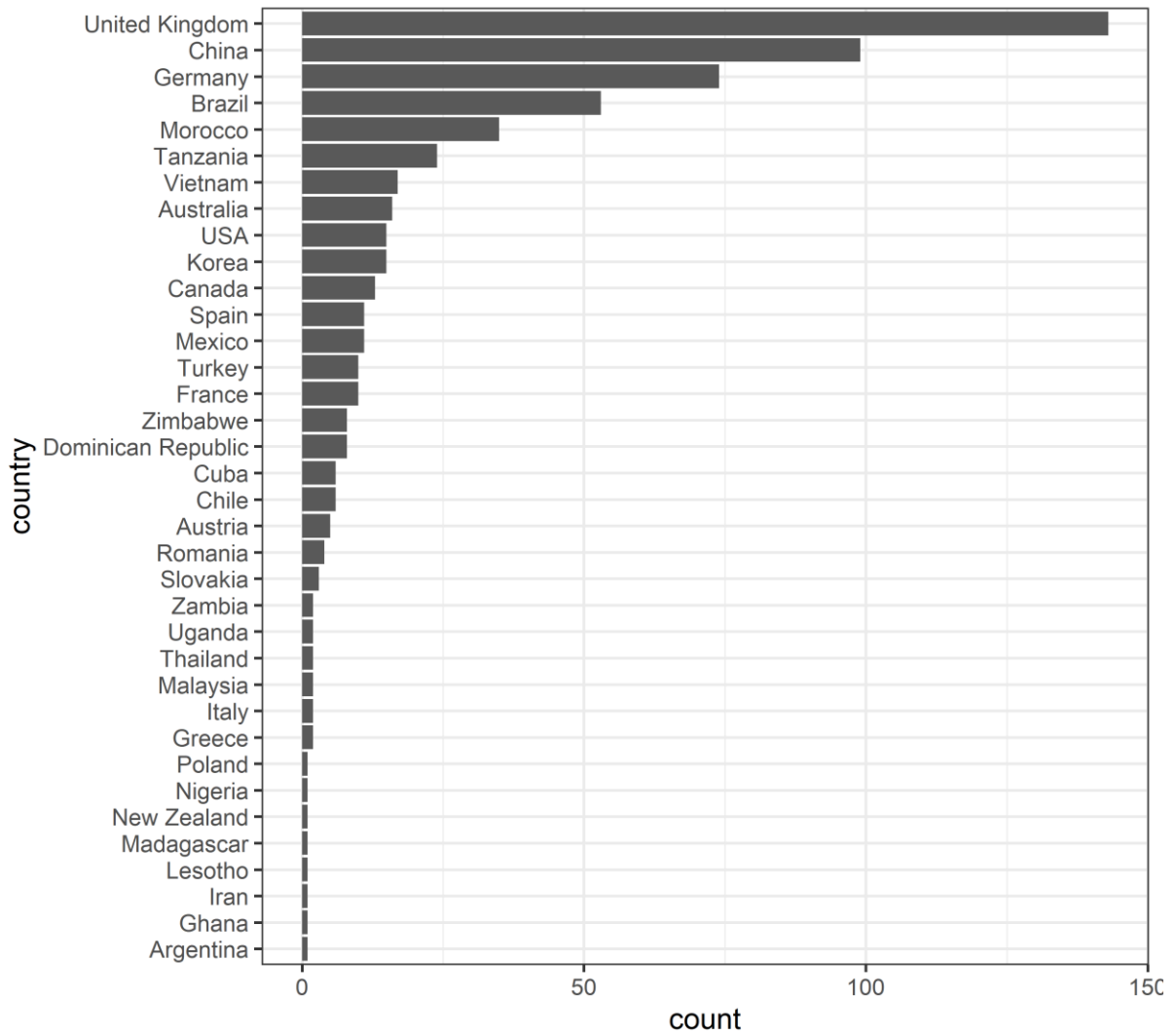


78

79 Figure S6: (a) Distribution of slope steepness (%) for measured erosion values (n = 606; Mean = 16 %; Median  
 80 = 11 %). (b) Distribution of annual precipitation (mm) for measured erosion values (n = 606; Mean = 879 mm;  
 81 Median = 774 mm). (c) Distribution of recorded measurement periods for soil loss experiments excluding  
 82 radioisotopic methods (n = 95; Mean = 15 a; Median = 1 a).

83

84

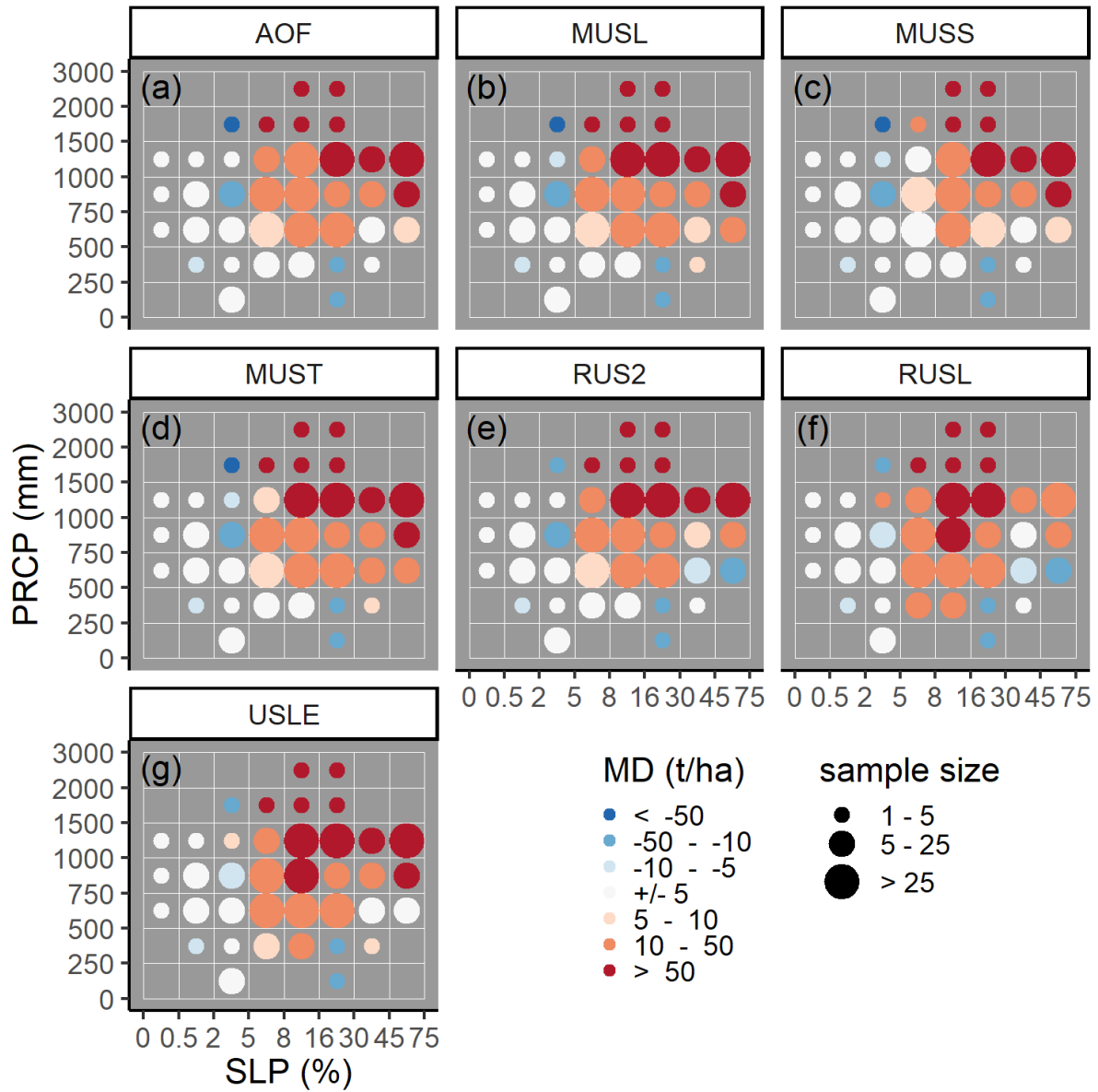


85

86 Figure S7: Number of measured water erosion records (n=606) per country (n=36).

87

88

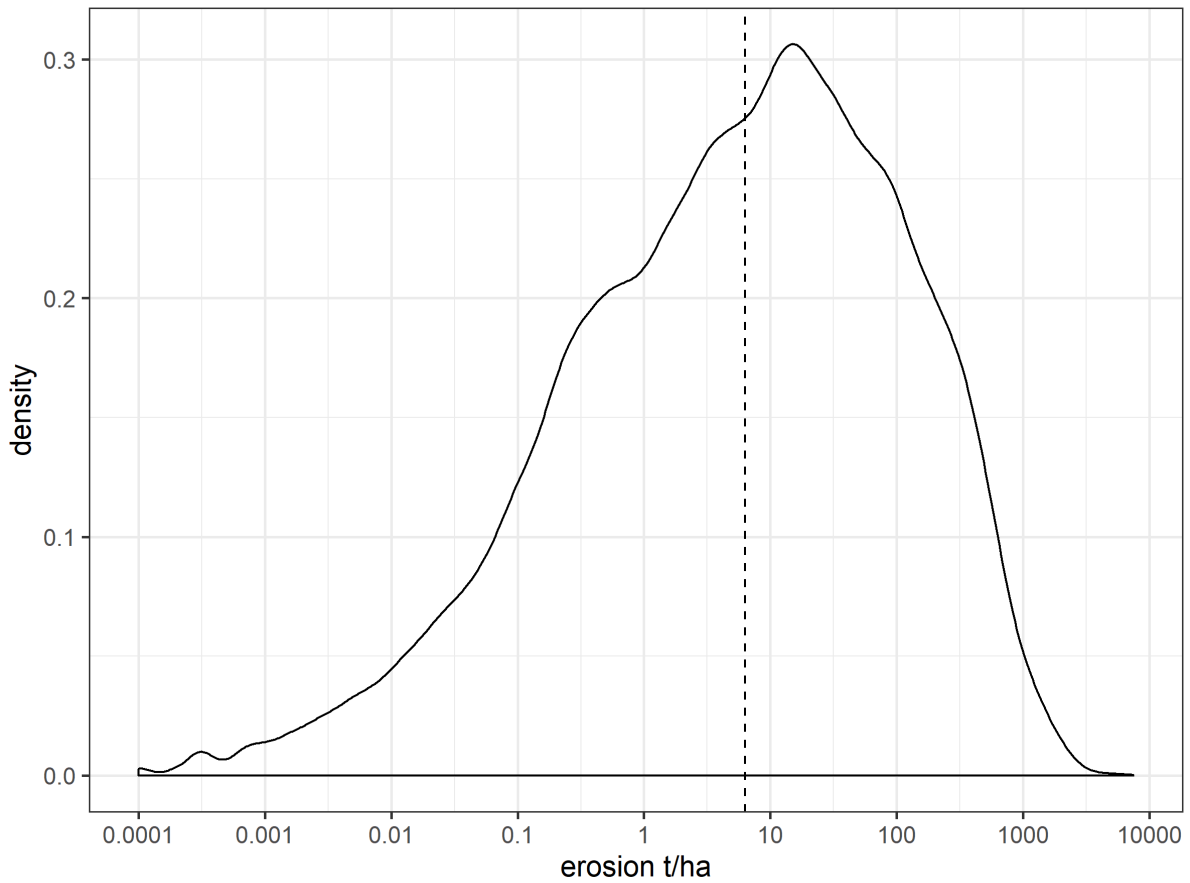


89

90 Figure S8: Median deviation (MD) in  $t\ ha^{-1}$  between measured and simulated water erosion using the baseline  
 91 scenario with different water erosion equations. Measured and simulated medians were calculated for different  
 92 slope and precipitation classes.

93

94



95

96 Figure S9: Distribution of average water erosion values from 1980 – 2010 simulated with the baseline scenario  
 97 and weighted for each simulation grid. The dashed vertical line illustrates the median of the distribution, which  
 98 represents global median water erosion of  $6 \text{ t ha}^{-1} \text{ a}^{-1}$ . Average water erosion at each grid and the global average  
 99 water erosion of  $19 \text{ t ha}^{-1} \text{ a}^{-1}$  has been calculated as a weighted average based on the distribution of irrigated and  
 100 rainfed maize and wheat acreage (Portmann et al., 2010).





101

102 Figure S10: Sugar cane cultivation on steep slopes in South China (Nanning, Guangxi Zhuang Autonomous  
103 Region). The steepest slopes are already abandoned and reforested by eucalyptus trees.

104



105

106 Figure S11: Cultivated slopes and rice terraces in South China (Nanning, Guangxi Zhuang Autonomous  
107 Region).





108

109 Figure S12: Maize cultivation on strongly eroded slopes (30 – 60 %) in South West Uganda (Kigwa, Kabale  
110 District).



111

112 Figure S13: Abandoned fields and maize cultivation on a steep slope (30 – 60 %) in South West Uganda  
113 (Kigwa, Kabale District).



114



115

116 Figure S14: Maize cultivation in South West Uganda (Kigwa, Kabale District).

117



118

119 Figure S15: Degraded and abandoned maize fields on steep slopes (20 – 60 %) in Northern El Salvador (San  
120 Ignacio, Chalatenango Department).

121





122

123 Figure S16: Degraded land in Northern El Salvador (Monte Redondo, Chalatenango Province).

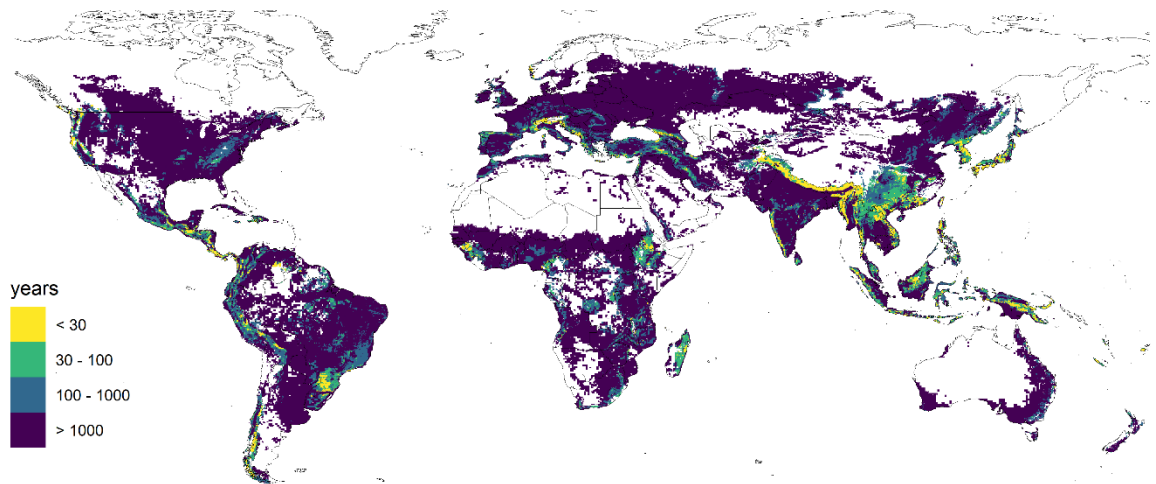
124



125

126 Figure S17: Gully erosion on arable land with slopes up to 20 – 30% in Slovakia (Figa, Rimavská Sobota  
127 District).

128

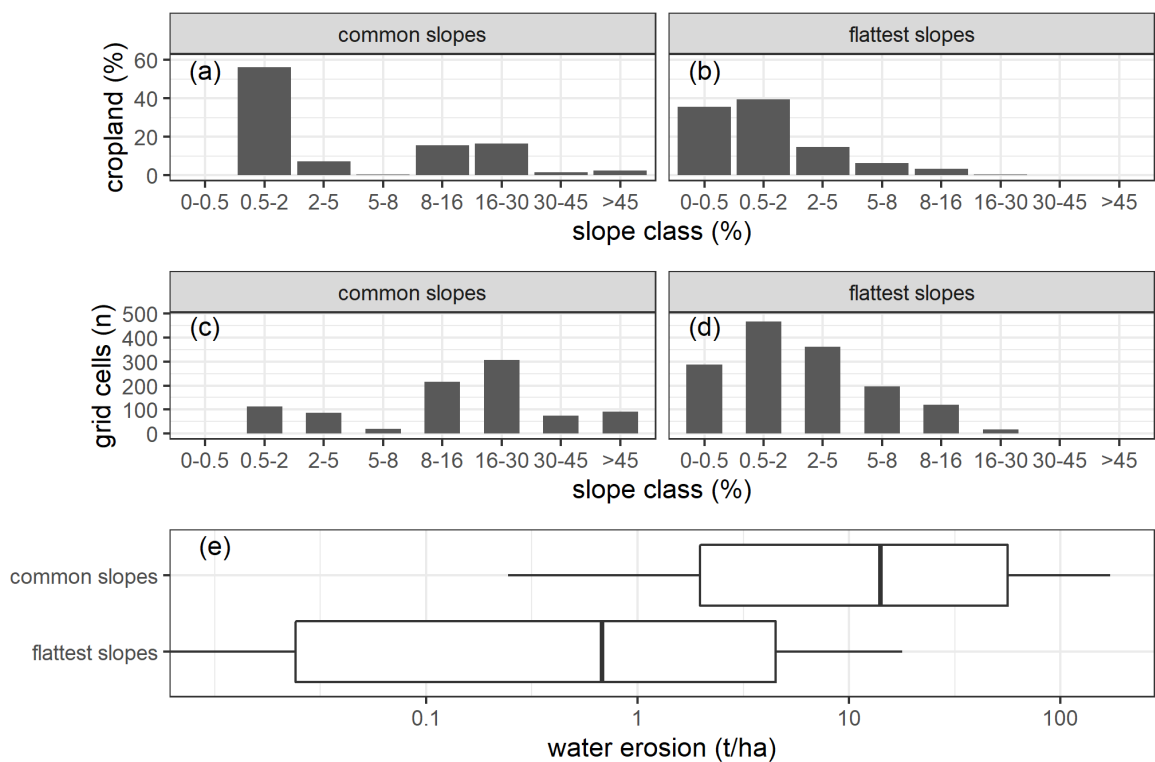


129

130 Figure S18: Simulated years left until the whole soil profile is eroded under permanent maize and wheat  
 131 cultivation. Calculated as a ratio of the sedimentary deposit thickness [m] (Pelletier et al., 2016) and the eroded  
 132 soil depth per year (water erosion [ $\text{t ha}^{-1} \text{a}^{-1}$ ] x bulk density [ $\text{g m}^{-3}$ ]).

133

134



135

136 Figure S19: Comparison of slope inputs and simulated water erosion outputs between the cropland distribution  
 137 scenario using the most common slopes and the cropland distribution scenario using the flattest terrain available  
 138 in Italy. (a, b) distribution of the cropland share (Portmann et al., 2010) per slope class. (c, d) distribution of grid  
 139 cells per slope class. (e) Simulated water erosion for Italy using both cropland distribution scenarios. Midlines  
 140 visualise median values, boxes include values from the 25th to the 75th percentiles and whiskers bracket values  
 141 between the 10th and the 90th percentiles.

142

143

144

Dominant slope class	Lower value (%)	Upper value (%)	Mid value (%)	Slope length (m)	Field size (ha)
1	0	0.5	0.25	200	10
2	0.5	2	1.25	200	10
3	2	5	3.5	200	10
4	5	8	6.5	200	10
5	8	16	12	100	5
6	16	30	18	75	5
7	30	45	35.5	50	1
8	45	100	60	20	1

145

146 Table S1. A set of rules for field size and slope length estimation for each dominant slope class. The  
 147 area/dominant slope class was assigned to each grid cell from a global slope and terrain dataset (Fisher et al.,  
 148 2007) providing 3 arc-sec spatial resolution distributions of nine slope gradient classes: 0–0.5%, 0.5–2%, 2–5%,  
 149 5–8%, 8–16%, 16–30%, 30–45%, and > 45% interpreted from SRTM elevation data (CGIAR-CSI, 2006). Mid-  
 150 interval value of the dominant slope class was used as an input for EPIC.

151 Table S2. Input parameters for the sensitivity analysis of the water erosion equations. Random values assigned  
 152 to each input parameter in the sensitivity analysis are defined by a range of discrete values or a triangular  
 153 distribution defined by the values given in the table.

154 Table S3. First- and total-order sensitivity indices (SI) ranking for 30 input parameters for each water erosion  
 155 equation.

156 Table S4. Spearman coefficients explaining the positive or negative correlation between the first- and total-order  
 157 sensitivity indices of the input parameters from each equation and the amount of annual rainfall at a location.

158 Table S5. Measured water erosion values collected from 113 studies. The reference list of each study is  
 159 available at TWCarr-si02.docx.

160

161